Supporting Information for

Optimization of Energy Levels by Molecular Design: Evaluation of *bis*-Diketopyrrolopyrrole Molecular Donor Materials for Bulk Heterojunction Solar cells.

By *Bright Walker, Jianhua Liu, Chunki Kim, Gregory C. Welch, Jin Keun Park, Jason Lin, Peter Zalar, Christopher M. Proctor, Jung Hwa Seo, Guillermo C. Bazan,* and *Thuc-Quyen Nguyen**

(This paper is dedicated to the memory of Mananya Tantiwiwat)

[*] Prof. T.-Q. Nguyen, Prof. G. Bazan, Dr. J. Liu, Dr. C. Kim, Dr. G. Welch, J. K. Park, J. Lin, P. Zalar, C. Proctor
Center for Polymers and Organic Solids and Department of Chemistry & Biochemistry
University of California at Santa Barbara, 93106, USA
E-mail: quyen@chem.ucsb.edu

Dr. B. Walker (Current address)
Interdisciplinary School of Green Energy
Ulsan National Institute of Science and Technology (UNIST)
Ulsan 689-798, Republic of Korea

Prof. J. H. Seo
Department of Materials Physics
Dong-A University
Busan 604-714, Republic of Korea

1. Material Synthesis and Characterization

Materials. Benzo[*b*]furan and chlorotrimethyltin were purchased from Alfa Aesar and used without any further purification. Benzofuran-2-boronic acid was purchased from Frontier Scientific and used as received. 5-hexyl-2,2'-bithiophene-5'-boronic acid pinacol ester, 2,1,3-benzothiadiazole-4,7-bis(boronic acid pinacol ester), Tris(dibenzylideneacetone)dipalladium, tetrakis(triphenylphosphine)palladium and other reagents were purchased from Sigma Aldrich and used as received. Toluene was dried over sodium/benzophenone and distilled at reduced pressure. Benzofuran-2-yl-trimethylstannane was synthesized according to a reported procedure.[1] Chloroform, tetrahydrofuran, and other solvents were used without any further purification. Flash chromatography was performed using Silicycle SiliaFlash® P60 (particle size 40-63 μm, 230-400 mesh) silica gel.

Characterization. Field desorption mass spectroscopy was carried out on a Waters GCT Premier high resolution time-of-flight mass spectrometer equipped with a field ionization/field desorption (FI/FD) ion sources. ^{1}H and ^{13}C nuclear magnetic resonance (NMR) spectroscopy spectra were recorded with a 400 MHz spectrometer (Varian, ASM-100) at 25 ºC using $CDCl_3$ as a solvent. Elemental analyses was recorded by a CEC 440HA Elemental Analyzer in UC Santa Barbara Marine Science Institute Analytical Laboratory.

All bisDPPs are synthesized by a divergent approach (Scheme S1), which involves a endcapping reaction via Suzuiki coupling. In the case of SDT bisDPP, the obtained product after suzuiki coupling possesses an unusual high polarity compared with other bisDPPs. It is reported that arylsilanes is easily cleaved by reaction with a nucleophile such as water[2] and SDT unit is liable to basic conditions.[3] We hypothesis the SDT unit undergoes a hydrolysis (Scheme S2) under the base and water condition that applied for Suzuki coupling, leading to a material with a hydrolyzed SDT core (SOHDT). This hypothesis is confirmed by the mass spectroscopy (**Fig. S1**) which shows has 18 Dalton higher than expected molecular weight. A further confirmation was conducted by synthesizing SDT bisDPP via Stille coupling as shown in Scheme A. Due to the mild condition of Stille coupling, the unhydrolyzed SDT bisDPP was successfully obtained and the mass spectroscopy shows the expected molecular weight (**Fig. S1**). Although the hydrolyzed SDT bisDPP was not the intended product, devices prepared using this material yielded superior performance compared to any of the other bis-DPP materials.

Scheme S1. Synthetic Route for BisDPP compounds.

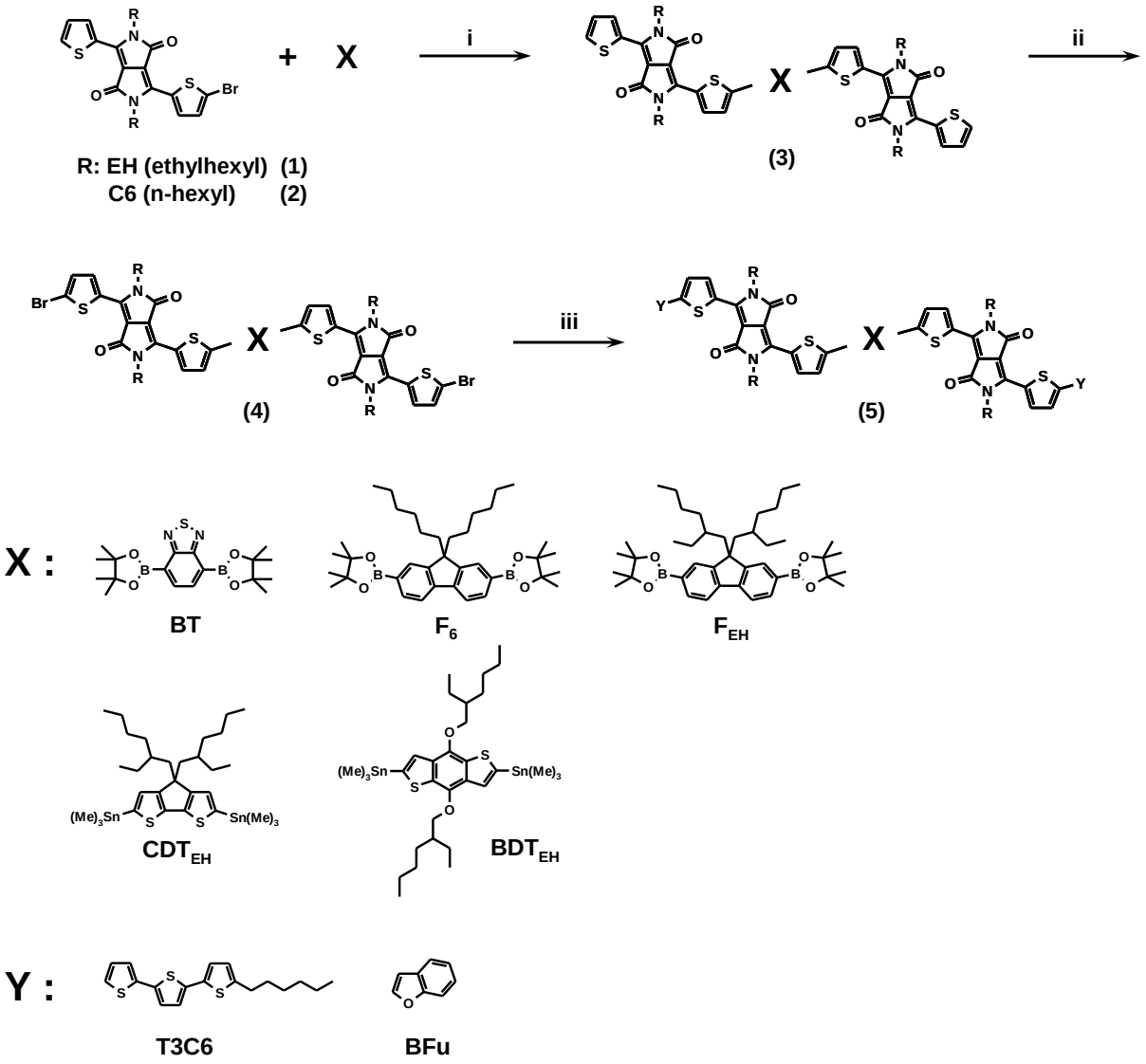

Conditions: (i) appropriate boronic acid pinacol ester, $Pd_2(dba)_3$, $HP(^tBu)_3BF_4$ (or PPh_3), K_3PO_4, THF (Suzuki coupling in conventional way) or appropriate trimethylstannyl compound, $Pd(PPh_3)_4$, xylene (microwave-assisted Stille coupling); (ii) NBS, $CHCl_3$; (iii) 5'-hexyl-2,2'-bithiophene-5-boronic acid pinacol ester (or benzofuran 2-boronic acid), $Pd_2(dba)_3$, $HP(^tBu)_3BF_4$ (or PPh_3), K_3PO_4 (or K_2CO_3), THF.

Scheme S2. Structural Abbreviations and Corresponding Molecular Structures of BisDPP Compounds.

$BDT_{EH}(TDPP_{EH}T)_2$

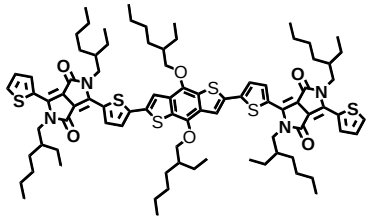

$BDT_{EH}(TDPP_{EH}TBFu)_2$

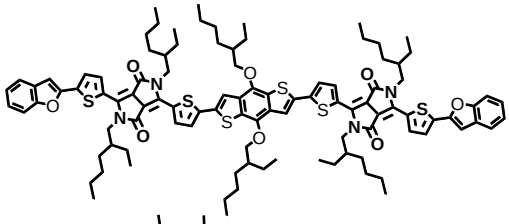

$BDT_{EH}(TDPP_{EH}TTT_{C6})_2$

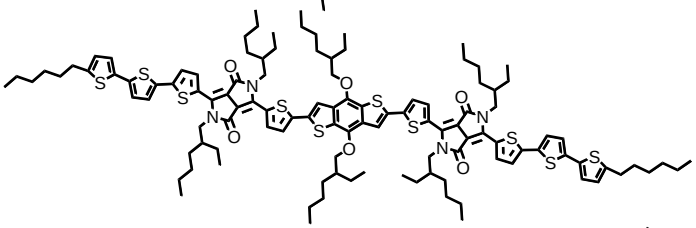

$BT(TDPP_{EH}TTT_{C6})_2$

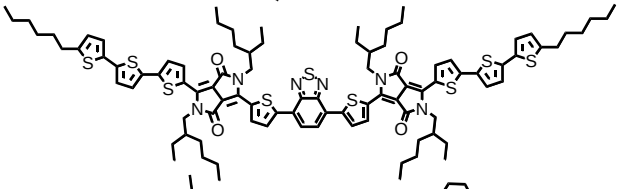

$F_{C6}(TDPP_{C6}TTT_{C6})_2$

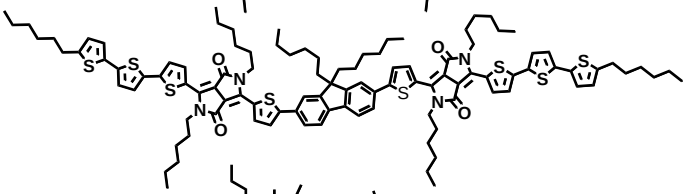

$F_{EH}(TDPP_{EH}TBFu)_2$

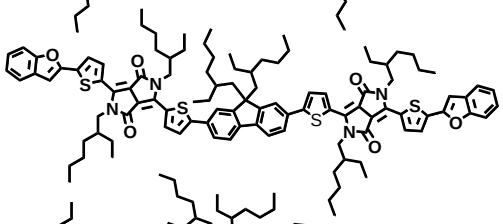

$SDT_{EH}(TDPP_{EH}TBFu)_2$

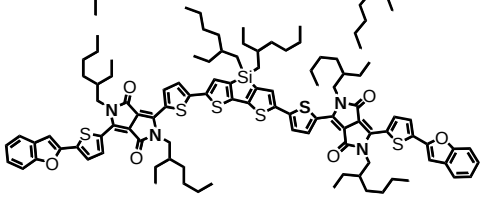

$SOHDT_{EH}(TDPP_{EH}TBFu)_2$

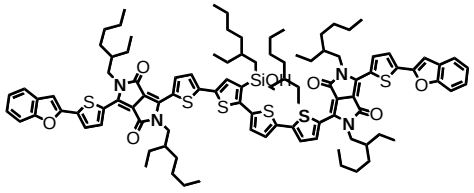

2,5-Bis(2-ethylhexyl)-3-(5-bromo-thiophene-2-yl)-6-(thiophene-2-yl)pyrrolo[3,4-c]pyrrole-1,4-dione, 1. To a solution of 2,5-bis(2-ethylhexyl)-3,6-di(thiophene-2-yl)-pyrrolo[3,4-c]pyrrole-1,4-dione[4](5.4 g, 18 mmol) in 130 mL of chloroform, N-bromosuccinimde (NBS) (2.1 g, 12 mmole) was added. The reaction solution was stirred for 5 hrs at room temperature in the dark. After adding more chloroform, solution was washed with waster and dried over magnesium sulfate. After solvent was removed under reduced pressure, the crude product was purified by column chromatography on a silica gel with chloroform/hexane from 1/1 to 2/1 (v/v) to afford **1** (3.5 g, 50 %). ^{1}H NMR (400 MHz, $CDCl_3$): 8.89 (d, 1H, J = 2.8 Hz), 8.62 (d, 1H, J = 3.6 Hz), 7.63 (d, 1H, J = 4.8 Hz), 7.26 (d, 1H, J = 4.0 Hz), 7.21 (d, 1H, J = 3.6 Hz), 3.88 - 4.05 (m, 4H), 1.84 (bs, 2H), 1.20 - 1.36 (m, 16H), 0.82 - 0.89 (m, 12H).

2,5-dihexyl-3-(5-bromo-thiophene-2-yl)-6-(thiophene-2-yl)pyrrolo[3,4-c]pyrrole-1,4-dione, 2. The procedure for **1** was followed to prepare **2** using 2,5-dihexyl-3,6-dithiophene-pyrrolo[3,4-c]pyrrole-1,4-dione[1] (1.7 g, 3.6 mmol) in 140 mL of chloroform. The crude product was purified by column chromatography on a silica gel with chloroform/hexane from 5/1 to 10/1 (v/v) to yield **2** (1.0 g, 73%). ^{1}H NMR (400 MHz, $CDCl_3$): 8.90 (d, 1H, J = 3.2 Hz), 8.63 (d, 1H, J = 3.6 Hz), 7.64 (d, 1H, J = 4.4 Hz), 7.28 (d, 1H, J = 4.0 Hz), 7.23 (d, 1H, J = 4.0 Hz), 3.93 - 4.04 (m, 4H), 1.84 (m, 4H), 1.20 - 1.36 (m, 12H), 0.82 - 0.89 (m, 6H).

4,7-Bis{5-[2,5-bis(2-ethylhexyl)-6-(thiophene-2-yl)pyrrolo[3,4-c]pyrrole-1,4-dione-3-yl]thiophene-2-yl}-2,1,3-benzothiadiazole, 3-1 (R = EH, X = BT). To a mixture of 2,1,3-benzothiadiazole-4,7-bis(boronic acid pinacol ester) (0.23 g, 0.60 mmol), **1** (0.90g, 1.5 mmol), tri(dibenzylidene-acetone)palladium (0) ($Pd_2(dba)_3$) (0.027 g, 0.030 mmol), tri-tert-butylphosphonium tetrafluoroborate (0.052 g, 0.18 mmol), and potassium phosphate (1.0 g, 4.8 mmol), degassed THF/water (20 mL/2mL) was added. After stirring under argon at 50 ^{o}C overnight, the reaction mixture was poured into water. The crude product was extracted by chloroform and dried over magnesium sulfate. After evaporate solvent, crude product was purified by column chromatography on a silica gel with pure chloroform to 1% (v/v) acetone in chloroform to afford desired product (0.5 g, 71 %). ^{1}H NMR (400 MHz, $CDCl_3$): 9.13 (d, 2H, J = 4.0 Hz), 8.96 (d, 2H, J = 4.0 Hz), 8.17 (d, 2H, J = 3.6 Hz), 8.01 (s, 2H), 7.63 (d, 2H, J = 5.2 Hz), 7.29 (d, 2H, J = 4.0 Hz), 4.04 - 4.16 (m, 8H), 2.00 (bs, 2H), 1.90 (bs, 2H), 1.25 - 1.46 (m, 32H), 0.86 - 0.98 (m, 24H).

9,9-dihexyl-2,7-Bis{5-[2,5-dihexyl-6-(thiophene-2-yl)pyrrolo[3,4-c]pyrrole-1,4-dione-3-yl]thiophene-2-yl}fluorene, 3-2 (R = C6, X = F_6). To a mixture of 9.9'-dihexyl-fluorene-2,7-boronic acid pinacol ester[2] (0.33, 0.56 mmol), **2** (0.70g, 1.3 mmol), $Pd_2(dba)_3$ (0.036g, 0.039 mmol), triphenylphosphine (0.061 g, 0.23 mmol), and potassium phosphate (1.9 g, 8.9 mmol),

degassed THF/water (18 mL/1.8mL) was added. After stirring under argon at 70 ^{o}C overnight, the reaction mixture was poured into water. The crude product was extracted by chloroform and dried over magnesium sulfate. After evaporate solvent, crude product was purified by column chromatography on a silica gel with pure chloroform to 1% (v/v) acetone in chloroform to afford desired product (0.66 g, 93 %). ^{1}H NMR (400 MHz, $CDCl_3$): 8.99 (d, 2H, J = 4.0 Hz), 8.93 (d, 2H, J = 3.2 Hz), 7.78 (d, 2H, J = 8.0 Hz), 7.70 (d, 2H, J = 8.0 Hz), 7.63 (d, 4H, J = 4.0 Hz), 7.55 (d, 2H, J = 4.0 Hz), 7.24 - 7.29 (m, 2H), 4.06 - 4.16 (m, 8H), 2.06 (m, 4H), 1.74 - 1.83 (m, 8H), 1.31 - 1.47 (m, 24H), 1.02 - 1.15 (m, 12H), 0.86 - 0.92 (m, 12H), 0.62 - 0.76 (m, 10H).

9,9-Bis(2-ethylhexyl)-2,7-bis{5-[2,5-bis(2-ethylhexyl)-6-(thiophene-2-yl)pyrrolo[3,4-c]pyrrole-1,4-dione-3-yl]thiophene-2-yl}fluorene, 3-3 (R = EH, X = F_{EH}). To a mixture of 9.9'-bis(2-ethylhexyl)-fluorene-2,7-boronic acid pinacol ester[2] (0.38, 0.58 mmol), **1** (0.80g, 1.3 mmol), $Pd_2(dba)_3$ (0.026g, 0.029 mmol), triphenylphosphine (0.045 g, 0.17 mmol), and potassium phosphate (2.0 g, 9.2 mmol), degassed THF/water (15 mL/1.5mL) was added. After stirring under argon at 70 ^{o}C overnight, the reaction mixture was poured into water. The crude product was extracted by chloroform and dried over magnesium sulfate. After evaporate solvent, crude product was purified by column chromatography on a silica gel with pure chloroform to 1% (v/v) acetone in chloroform to afford desired product (0.60 g, 72 %). ^{1}H NMR (400 MHz, $CDCl_3$): 9.08 (q, 2H), 8.92 (d, 2H, J = 4.0 Hz), 7.79 (d, 2H, J = 8.0 Hz), 7.70 (t, 4H) 7.65 (d, 2H, J = 5.2 Hz), 7.54 (m, 2H), 7.30 (m, 2H), 4.06 - 4.16 (m, 8H), 2.11 (bs, 4H), 2.00 (m, 2H), 1.90 (m, 2H), 1.20 - 1.47 (m, 32H), 0.72 - 0.98 (m, 42H), 0.55 - 0.68 (m, 12H).

4,4-Bis(2-ethylhexyl)-2,6-bis{5-[2,5-bis(2-ethylhexyl)-6-(thiophene-2-yl)pyrrolo[3,4-c]pyrrole-1,4-dione-3-yl]thiophene-2-yl}dithieno[3,2-b;2',3'-d]silole, 3-4 (R = EH, X = SDT_{EH}). 2,6-bis(trimethylstannyl)-4,4'-bis(2-ethylhexyl)dithieno[3,2-b:2',3'-d]silole (0.24 g, 0.41 mmol), tetrakis(triphenylphosphine)palladium (0) ($Pd(PPh_3)_4$) (0.025 g, 0.020 mmol), and **1** (0.50 g, 0.83 mmol), and 15 mL of toluene were placed in a 20 mL microwave tube. The reaction mixture was heated to 120 ^{o}C for 1 minute, 140 ^{o}C for 1 minute, 160 ^{o}C for 1 minute and 175 ^{o}C for 60 minutes, using a Biotage microwave reactor. The solid was slurried in methanol, sonicated for 2 minutes, and filtered. The solid was washed with methanol and dried under vacuum. The crude product was purified by column chromatography on a silica gel with pure chloroform to 1% (v/v) acetone in chloroform to obtain desired product (0.45 g, 75 %). ^{1}H NMR (400 MHz, $CDCl_3$): 8.98 (d, 2H, J = 4.0 Hz), 8.89 (d, 2H, J = 4.0 Hz), 7.61 (d, 2H, J = 4.4 Hz), 7.29 (t, 4H), 7.25 (d, 2H, J = 4.0 Hz), 4.05 (m, 8H), 1.82 - 1.97 (m, 4H), 1.18 - 1.50 (m, 50H), 1.02 (t, 4H, J = 6.4 Hz), 0.79 - 0.94 (m, 36H).

4,4-Bis(2-ethylhexyl)-2,6-bis{5-[2,5-bis(2-ethylhexyl)-6-(thiophene-2-yl)pyrrolo[3,4-c]pyrrole-1,4-dione-3-yl]thiophene-2-yl}cyclopenta[2,1-b:3,4-b']dithiophene, 3-5 (R = EH, X = CDT_{EH}). The procedure for **3-4** was followed to prepare **3-5** using2,6-(trimethylstannyl)-4,4-bis(dodecil)-4H-cyclopenta[2,1-b;3,4-b']dithiophene (344 mg, 0.41 mmol), instead of 2,6-bis(trimethylstannyl)-4,4'-bis(2-ethylhexyl)dithieno[3,2-b:2',3'-d]silole. The crude product was purified by column chromatography on a silica gel with chloroform to yield desired product (0.51 g, 79 %). ^{1}H NMR (400 MHz, $CDCl_3$): 8.91 (d, 2H, *J* = 4.0 Hz), 8.89 (d, 2H, *J* = 4 Hz), 7.62 (d, 2H, *J* = 4.8 Hz), 7.32 (d, 2H, *J* = 4.0 Hz), 7.28 (d, 2H, *J* = 4.8 Hz), 7.20 (s, 2H), 4.06 (m, 8H), 1.91 (m, 8H), 1.39 (m, 14H), 1.33 (m, 12H), 1.24 (m, 48H), 1.03 (m, 4H), 0.89 (m 34H).

4,8-Bis(2-ethylhexyloxy)-2,6-bis{5-[2,5-bis(2-ethylhexyl)-6-(thiophene-2-yl)pyrrolo[3,4-c]pyrrole-1,4-dione-3-yl]thiophene-2-yl}benzo[1,2-b:4,5-b']dithihophene, 3-6 (R = EH, X = BDT_{EH}). The procedure for **3-4** was followed to prepare **3-6** using 4,8-bis(2-ethylhexyloxy)-2,6-bis(trimethylstannyl)benzo[1,2-b:4,5-b']dithiophene (0.29 g, 0.38 mmol), instead of 2,6-bis(trimethylstannyl)-4,4'-bis(2-ethylhexyl)dithieno[3,2-b:2',3'-d]silole. The crude product was purified by column chromatography on a silica gel with chloroform to yield desired product (0.37 g, 66 %). ^{1}H NMR (400 MHz, $CDCl_3$): 9.01 (d, 2H, *J* = 4.0 Hz), 8.94 (d, 2H, *J* = 4.0 Hz), 7.63 (d, 2H, *J* = 3.6 Hz), 7.61 (s, 2H), 7.40 (d, 2H, *J* = 4.0 Hz), 7.28 (d, 2H, *J* = 4.0 Hz), 4.21 (d, 4H, *J* = 5.2 Hz), 4.07 (m, 8H), 1.82 - 1.96 (m, 6H), 1.60 - 1.79 (m, 4H), 1.25 - 1.56 (m, 44H), 1.07 (t, 6H, *J* = 7.2 Hz), 0.85 - 1.00 (m, 30H). FD-TOF MS (m/z): calc'd for $C_{86}H_{114}N_4O_6S_6$ [M^+] 1490.71; found 1490.6.

4,7-Bis{5-[2,5-bis(2-ethylhexyl)-6-(5-bromo-thiophene-2-yl)pyrrolo[3,4-c]pyrrole-1,4-dione-3-yl]thiophene-2-yl}-2,1,3-benzothiadiazole, 4-1 (R = EH, X = BT). NBS (0.16 g, 0.88 mmol) was added to a solution of **3-1** (0.50 g, 0.42 mmol) in 40 mL of chloroform. The solution was stirred overnight in the dark. The solution was diluted with additional chloroform and washed with water. After evaporate solvent under reduced pressure, the crude product was purified by column chromatography on a silica gel with chloroform/hexane from 10/1 to 30/1 (v/v) to yield desired product (0.35 g, 62 %). ^{1}H NMR (400 MHz, $CDCl_3$): 9.11 (d, 2H, *J* = 2.8 Hz), 8.70 (d, 2H, *J* = 4.0 Hz), 8.07 (d, 2H, *J* = 4.0 Hz), 7.89 (d, 2H), 7.17 (d, 2H, *J* = 4.0 Hz), 3.85 - 4.14 (m, 8H), 1.97 (bs, 2H), 1.86 (bs, 2H), 1.28 - 1.44 (m, 32H), 0.87 - 0.97 (m, 24H).

9,9-Dihexyl-2,7-bis{5-[2,5-dihexyl-6-(5-bromo-thiophene-2-yl)pyrrolo[3,4-c]pyrrole-1,4-dione-3-yl]thiophene-2-yl}fluorene, 4-2 (R = C6, X = F_6). The procedure for **4-1** was followed to prepare **4-2** using **3-2** (0.60 g, 0.47 mmol) in 30 mL of chloroform. The crude product was purified by column chromatography on a silica gel with chloroform/hexane from 5/1 to 10/1 (v/v) to yield desired product (0.53 g, 79 %). ^{1}H NMR (400 MHz, $CDCl_3$): 9.00 (d, 2H, *J* = 4.4 Hz),

8.60 (d, 2H, *J* = 4.0 Hz), 7.74 (d, 2H, *J* = 8.0 Hz), 7.68 (d, 2H, *J* = 8.0 Hz), 7.62 (s, 2H), 7.54 (d, 2H, *J* = 4.0 Hz), 7.22 (d, 2H, *J* = 4.4 Hz), 4.13 (t, 4H, *J* = 7.2 Hz), 4.00 (t, 4H, *J* = 8.0 Hz), 2.06 (m, 4H), 1.68 - 1.83 (m, 8H), 1.31 - 1.50 (m, 24H), 1.00 - 1.15 (m, 12H), 0.86 - 0.92 (m, 12H), 0.62 - 0.76 (m, 10H).

9,9-Bis(2-ethylhexyl)-2,7-bis{5-[2,5-bis(2-ethylhexyl)-6-(5-bromo-thiophene-2-yl)pyrrolo[3,4-c]pyrrole-1,4-dione-3-yl]thiophene-2-yl}fluorene, 4-3 (R = EH, X = F_{EH}). The procedure for **4-1** was followed to prepare **4-3** using **3-3** (0.60 g, 0.42 mmol) in 40 mL of chloroform. The crude product was purified by column chromatography on a silica gel with chloroform/hexane from 5/1 to 10/1 (v/v) to yield desired product (0.44 g, 66 %). ^{1}H NMR (400 MHz, $CDCl_3$): 9.08 (q, 2H), 8.92 (d, 2H, *J* = 4.0 Hz), 7.79 (d, 2H, *J* = 8.0 Hz), 7.70 (t, 4H), 7.54 (m, 2H), 7.21 (d, 2H, *J* = 4.0 Hz), 4.06 - 4.16 (m, 8H), 2.11 (bs, 4H), 2.00 (m, 2H), 1.90 (m, 2H), 1.20 - 1.47 (m, 32H), 0.72 - 0.98 (m, 42H), 0.55 - 0.68 (m, 12H).

4,4-Bis(2-ethylhexyl)-2,6-bis{5-[2,5-bis(2-ethylhexyl)-6-(5-bromo-thiophene-2-yl)pyrrolo[3,4-c]pyrrole-1,4-dione-3-yl]thiophene-2-yl}dithieno[3,2-b;2',3'-d]silole, 4-4 (R = EH, X = SDT_{EH}). The procedure for **4-1** was followed to prepare **4-4** using **3-4** (0.70 g, 0.48 mmol) in 20 mL of chloroform. The crude product was purified by column chromatography on a silica gel with chloroform/hexane from 5/1 to 10/1 (v/v) to yield desired product (0.58 g, 74 %). ^{1}H NMR (400 MHz, $CDCl_3$): 8.98 (d, 2H, *J* = 4.4 Hz), 8.53 (d, 2H, *J* = 4.0 Hz), 7.28 (s, 2H), 7.12 (d, 4H, *J* = 4.0 Hz), 3.87 - 4.08 (m, 8H), 1.78 - 1.95 (m, 4H), 1.53 (m, 2H), 1.15 - 1.43 (m, 48H), 1.06 (t, 4H, *J* = 6.4 Hz), 0.80 - 0.95 (m, 36H).

4,8-Bis(2-ethylhexyloxy)-2,6-bis{5-[2,5-bis(2-ethylhexyl)-6-(5-bromo-thiophene-2-yl)pyrrolo[3,4-c]pyrrole-1,4-dione-3-yl]thiophene-2-yl}benzo[1,2-b:4,5-b']dithihophene, 4-5 (R = EH, X = BDT_{EH}). The procedure for **4-1** was followed to prepare **4-5** using **3-5** (0.25 g, 0.17 mmol) in 12 mL of chloroform. The crude product was purified by column chromatography on a silica gel with chloroform/hexane from 5/1 to 30/1 (v/v) to yield desired product (0.16 g, 57 %). ^{1}H NMR (400 MHz, $CDCl_3$): 9.00 (d, 2H, *J* = 4.0 Hz), 8.68 (d, 2H, *J* = 4.0 Hz), 7.50 (s, 2H), 7.38 (d, 2H, *J* = 4.0 Hz), 7.18 (d, 2H, *J* = 4.0 Hz), 3.85 - 4.21 (m, 12H), 1.60 - 1.96 (m, 10H), 1.18 - 1.56 (m, 44H), 0.85 - 1.07 (m, 36H).

4,7-Bis{2-[2,5-bis(2-ethylhexyl)-6-(5-hexyl-2,2':5',2''-terthiophene-5''-yl)pyrrolo[3,4-c]pyrrolo-1,4-dione-3-yl]-thiophene-5-yl}-2,1,3-benzothiadiazole, 5-1 (R = EH, X = BT, Y = T3C6). Degassed THF/water (10 mL/1mL) was added to a mixture of **4-1** (0.35 g, 0.26 mmol),

5-hexyl-2,2'-bithiophene-5'-boronic acid pinacol ester (0.24 g, 0.64 mmol), $Pd_2(dab)_3$ (0.012 g, 0.013 mmol), tri-tert-butylphosphonium tetrafluoroborate (0.023 g, 0.79 mmol), and potassium phosphate (0.44 g, 2.1 mmol). After stirring overnight under argon at 60 ^oC, the reaction mixture was poured into water. The crude product was extracted with chloroform and purified by column chromatography on a silica gel with chloroform to 1 % (v/v) acetone in chloroform pure chloroform to obtain desired product (0.22 g, 50%). ^1H NMR (400 MHz, $CDCl_3$): 9.03 (s, 2H), 8.97 (s, 2H), 7.90 (s, 2H), 7.71 (s, 2H), 7.06 (d, 2H, J = 3.6 Hz), 6.98 (d, 2H, J = 4.0 Hz), 6.88 (d, 2H, J = 3.2 Hz), 6.84 (d, 2H, J = 3.6 Hz), 6.58 (d, 2H, J = 3.2 Hz), 3.78 - 4.05 (m, 8H), 2.68 (t, 4H, J = 7.2 Hz), 1.82 - 1.98 (m, 4H), 1.61 (m, 4H), 1.21 - 1.50 (m, 44H), 0.86 - 1.02 (m, 30H). Anal. Calcd. for $C_{94}H_{112}N_6O_4S_9$ (%): C, 67.26; H, 6.73; N, 5.01. Found: C, 66.78; H, 6.69; N, 5.11. FD-TOF MS (m/z): calc'd for $C_{94}H_{112}N_6O_4S_9$ [M^+] 1676.62; found 1676.5.

9,9-Dihexyl-2,7-bis{5-[2,5-dihexyl-6-(5-hexyl-2,2':5',2''-terthiophene-5''-yl)pyrrolo[3,4-c]pyrrole-1,4-dione-3-yl]thiophene-2-yl}fluorene, 5-2 (R = C6, X = F_6, Y = T3C6). To a mixture of **4-2** (0.50 g, 0.35 mmol), 5-hexyl-2,2'-bithiophene-5'-boronic acid pinacol ester (0.40 g, 1.1 mmol), $Pd_2(dba)_3$ (0.032 g, 0.035 mmol), triphenylphosphine (0.055 g, 0.21 mmol), and potassium carbonate (0.78 g, 5.6 mmol), degassed THF/water (14 mL/1.4 mL) was added. After stirring overnight under argon at 70 ^oC, the reaction mixture was poured into water. The crude product was extracted with chloroform and purified by column chromatography on a silica gel with from chloroform/hexane from 10/1 to 30/1 (v/v) to obtain desired product (0.37 g, 60%). ^1H NMR (400 MHz, $CDCl_3$): 8.99 (d, 2H, J = 4.0 Hz), 8.93 (d, 2H, J = 3.2 Hz), 7.75 (d, 2H, J = 8.0 Hz), 7.70 (d, 2H, J = 8.0 Hz), 7.63 (s, 2H), 7.55 (d, 2H, J = 4.0 Hz), 7.30 (d, 2H, J = 4.0 Hz), 7.23 (d, 2H, J = 4.0 Hz), 7.04 (m, 4H), 6.71 (d, 2H, J = 4.0 Hz), 4.08 (m, 8H), 2.81 (t, 4H, J = 7.6 Hz), 2.06 (m, 4H), 1.74 - 1.86 (m, 8H), 1.70 (m, 4H), 1.31 - 1.47 (m, 36H), 1.02 - 1.18 (m, 12H), 0.86 - 0.92 (m, 18H), 0.62 - 0.76 (m, 10H). Anal. Calcd. for $C_{105}H_{126}N_4O_4S_8$ (%): C, 71.47; H, 7.20; N, 3.17 Found: C, 71.05; H, 7.08; N, 3.32. FD-TOF MS (m/z): calc'd for $C_{105}H_{126}N_4O_4S_8$ [M^+] 1762.75; found 1762.6.

9,9-Bis(2-ethylhexyl)-2,7-bis{5-[2,5-bis(2-ethylhexyl)-6-[5-(benzofuran-2-yl)thiophene-2-yl]pyrrolo[3,4-c]pyrrole-1,4-dione-3-yl]thiophene-2-yl}fluorene, 5-3 (R = EH, X = F_{EH}, Y = BFu). To a mixture of **4-3** (0.35 g, 0.22 mmol), benzofuran-2-boronic acid (0.11 g, 0.66 mmol), $Pd_2(dba)_3$ (0.010 g, 0.011 mmol), tri-tert-butylphosphonium tetrafluoroborate (0.019 g, 0.066 mmol), and potassium phosphate (0.75 g, 3.5 mmol), degassed THF/water (7 mL/0.7 mL) was added. After stirring overnight under argon at 70 ^oC, the reaction mixture was poured into water. The crude product was extracted with chloroform and purified by column chromatography on a silica gel with from chloroform/hexane from 10/1 to 30/1 (v/v) to obtain desired product (0.22 g, 60%). ^1H NMR (400 MHz, $CDCl_3$): 9.08 (q, 2H), 9.00 (d, 2H, J = 4.0 Hz), 7.77 (d, 2H, J = 8.0 Hz), 7.70 (t, 4H), 7.60 (t, 4H), 7.53 (m, 4H), 7.34 (t, 2H, J = 7.2 Hz), 7.28 (t, 2H, J = 7.2 Hz),

7.07 (s, 2H), 4.12 (m, 8H), 2.11 (bs, 4H), 2.00 (m, 4H), 1.25 - 1.47 (m, 32H), 0.72 - 0.98 (m, 42H), 0.52 - 0.68 (m, 12H). Anal. Calcd. for $C_{105}H_{126}N_4O_6S_4$ (%): C, 75.59; H, 7.61; N, 3.36 Found: C, 75.90; H, 7.45; N, 3.11. FD-TOF MS (m/z): calc'd for $C_{105}H_{126}N_4O_6S_4$ [M^+] 1666.86; found 1666.7.

4,8-Bis(2-ethylhexyloxy)-2,6-bis{5-[2,5-bis(2-ethylhexyl)-6-(5-hexyl-2,2':5',2"-terthiophene-5"-yl)pyrrolo[3,4-c]pyrrole-1,4-dione-3-yl]thiophene-2-yl}benzo[1,2-b:4,5-b']dithihophene, 5-5 (R = EH, X = BDT_{EH}, Y = T3C6). To a mixture of **4-5** (0.16 g, 0.097 mmol), 5-hexyl-2,2'-bithiophene-5'-boronic acid pinacol ester (0.11 g, 0.29 mmol), $Pd_2(dba)_3$ (0.009 g, 0.010 mmol), triphenylphosphine (0.015 g, 0.058 mmol), and potassium phosphate (0.33 g, 1.6 mmol), degassed THF/water (6 mL/0.6 mL) was added. After stirring overnight under argon at 70 ^oC, the reaction mixture was poured into water. The crude product was extracted with chloroform and purified by column chromatography on a silica gel with from chloroform/hexane from 10/1 (v/v) to chloroform to obtain desired product (0.10 g, 53%). ^1H NMR (400 MHz, $CDCl_3$): 9.06 (d, 2H, J = 4.0 Hz), 9.01 (d, 2H, J = 4.0 Hz), 7.29 (s, 2H), 7.20 (d, 2H, J = 4.4 Hz), 7.10 (d, 4H, J = 4.4 Hz), 7.01 (d, 2H, J = 3.6 Hz), 6.91 (d, 2H, J = 3.2 Hz), 6.86 (d, 2H, J = 3.6 Hz), 6.62 (d, 2H, J = 3.6 Hz), 3.87 - 4.12 (m, 12H), 2.72 (t, 4H, J = 7.6 Hz), 1.59 - 1.95 (m, 14H), 1.21 - 1.50 (m, 56H), 1.12 (t, 6H, J = 7.6 Hz), 0.80 - 1.05 (m, 36H). Anal. Calcd. for $C_{114}H_{146}N_4O_6S_{10}$ (%): C, 68.84; H, 7.40; N, 2.82 Found: C, 68.38; H, 7.16; N, 3.03. FD-TOF MS (m/z): calc'd for $C_{114}H_{146}N_4O_6S_{10}$ [M^+] 1986.84; found 1986.7.

Scheme S2. Synthetic route of bis-DPP using a SDT core.

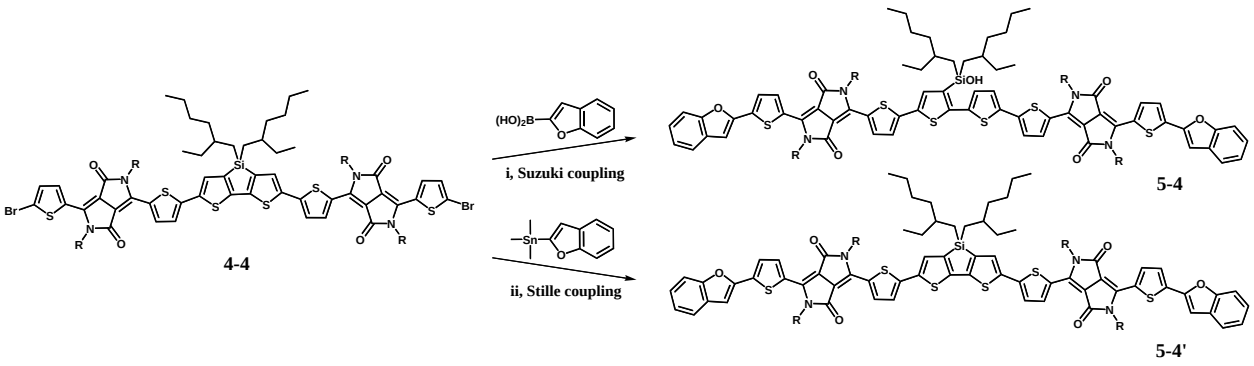

Conditions: (i) $Pd_2(dba)_3$, $HP(^tBu)_3BF_4$ (or PPh_3), K_3PO_4, THF/H_2O (Suzuki coupling); (ii) $Pd(PPh_3)_4$, xylene (microwave-assisted Stille coupling).

3-[bis(2-ethylhexyl)silanol-yl]-5,5'-bis{5-[2,5-bis(2-ethylhexyl)-6-[5-(benzofuran-2-yl)thiophene-2-yl]pyrrolo[3,4-c]pyrrole-1,4-dione-3-yl]-2,2'-bithiophene, 5-4 (R = EH, X = $SOHDT_{EH}$, Y = BFu). To a mixture of **4-4** (0.58 g, 0.36 mmol), benzofuran-2-boronic acid (0.17 g, 1.1 mmol), $Pd_2(dba)_3$ (0.016 g, 0.018 mmol), tri-tert-butylphosphonium tetrafluoroborate (0.031 g, 0.107 mmol), and potassium phosphate (1.21 g, 5.7 mmol), degassed THF/water (12 mL/1.2 mL) was added. After stirring overnight under argon at 70 ^{o}C, the reaction mixture was poured into water. The crude product was extracted with chloroform and purified by column chromatography on a silica gel with from chloroform/hexane from 10/1 to 30/1 (v/v) to obtain desired product (0.36 g, 59%). ^{1}H NMR (400 MHz, $CDCl_3$): 8.97 (m, 4H), 7.55 (m, 4H), 7.49 (d, 2H, *J* = 8 Hz), 7.36 (t, 1H, *J* = 7.2 Hz), 7.30 (t, 3H), 7.22 (m, 5H), 7.01 (s, 2H), 3.92-4.12 (m, 8H), 2.63 (t, 1H), 1.93 (m, 4H), 1.15-1.48 (m, 50H), 0.80-0.95 (m, 40H). Anal. Calcd. for $C_{100}H_{124}N_4O_7S_6Si$ (%): C, 70.05; H, 7.29; N, 3.27 Found: C, 70.32; H, 7.11; N, 3.19. FD-TOF MS (m/z): calc'd for $C_{100}H_{124}N_4O_7S_6Si$ [M^+] 1713.7; found 1713.7.

4,4-Bis(2-ethylhexyl)-2,6-bis{5-[2,5-bis(2-ethylhexyl)-6-[5-(benzofuran-2-yl)thiophene-2-yl]pyrrolo[3,4-c]pyrrole-1,4-dione-3-yl]thiophene-2-yl}dithieno[3,2-b;2',3'-d]silole, 5-4' (R = EH, X = SDT_{EH}, Y = BFu). Compound **4-4** (0.65 g, 0.40 mmol), tetrakis(triphenylphosphine) palladium (0) ($Pd(PPh_3)_4$) (0.025 g, 0.020 mmol), and (benzofuran-2-yl)trimethylstannane (0.25 g, 0.88 mmol), and 15 mL of toluene were placed in a 20 mL microwave tube. The reaction mixture was heated to 80 ^{o}C for 2 minute, 120 ^{o}C for 2 minute, 140 ^{o}C for 2 minute, 160 ^{o}C for 2 minute and 175 ^{o}C for 40 minutes, using a Biotage microwave reactor. The solid was slurried in methanol, sonicated for 2 minutes, and filtered. The solid was washed with methanol and dried under vacuum. The resulting curde product was purified by column chromatography on a silica gel using a mixture of chloroform and hexane as an eluent. 0.51 g of purified product was obtained (76% yield). ^{1}H NMR (400 MHz, $CDCl_3$): 8.98 (d, 2H, *J* = 4.0 Hz), 8.84 (d, 2H, *J* = 4.0 Hz), 7.46 (d, 2H, *J* = 8.0 Hz), 7.39 (d, 2H, *J* = 8.0 Hz), 7.33-7.20 (m, 8H), 6.96 (s, 2H), 6.80 (s, 2H), 4.08 (m, 8H), 1.82-1.97 (m, 6H), 1.52-1.18 (m, 50H), 1.02-0.80 (m, 36H). Anal. Calcd. for $C_{100}H_{122}N_4O_6S_6Si$ (%): C, 70.80; H, 7.25; N, 3.30 Found: C, 70.51; H, 7.16; N, 3.39. FD-TOF MS (m/z): calc'd for $C_{46}H_{48}N_2O_2S_4$ [M^+] 1695.75; found 1695.7.

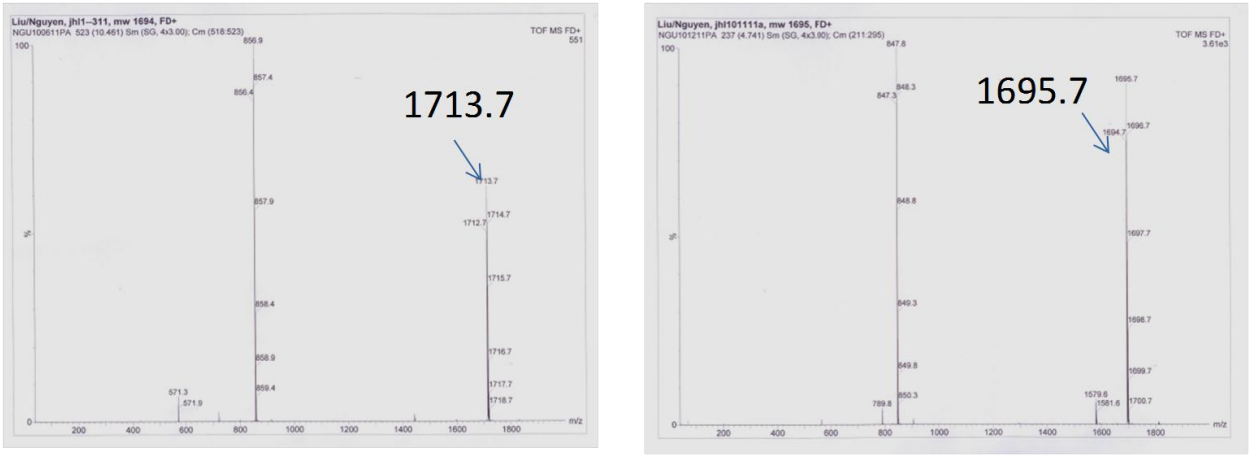

Figure S1. Field-desorption time-of-flight mass spectroscopy of hydrolyzed SDT bisDPP (left) and SDT bisDPP (right).

2. Optical and electronic properties of bis-DPP compounds

2.1 UV-vis Absorption Spectra

Absorption spectra were collected for both solutions (approx. 5-10 μg/mL in $CHCl_3$) and films (spin cast from ~2 mg/mL solutions in $CHCl_3$ at 2000 rpm) of each material and are plotted in **Figure S2**. Materials exhibit absorption onsets in the range of 660 – 820 nm in solution and 720 – 960 as films. All materials show a broadening and red-shift of the absorption spectra going from solution to film, indicating some level of aggregation and electronic delocalization in the solid state. The broadening and red-shift for $BT(TDPP_{EH}TTT_{C6})_2$ (140 nm) is considerably larger than the other materials (53 to 97 nm). It would appear that the BT unit leads to extensive packing and delocalization in the solid state compared to other core groups. The average red-shift of absorption onset for the remaining materials is found to be 70 nm with a standard deviation of 14 nm.

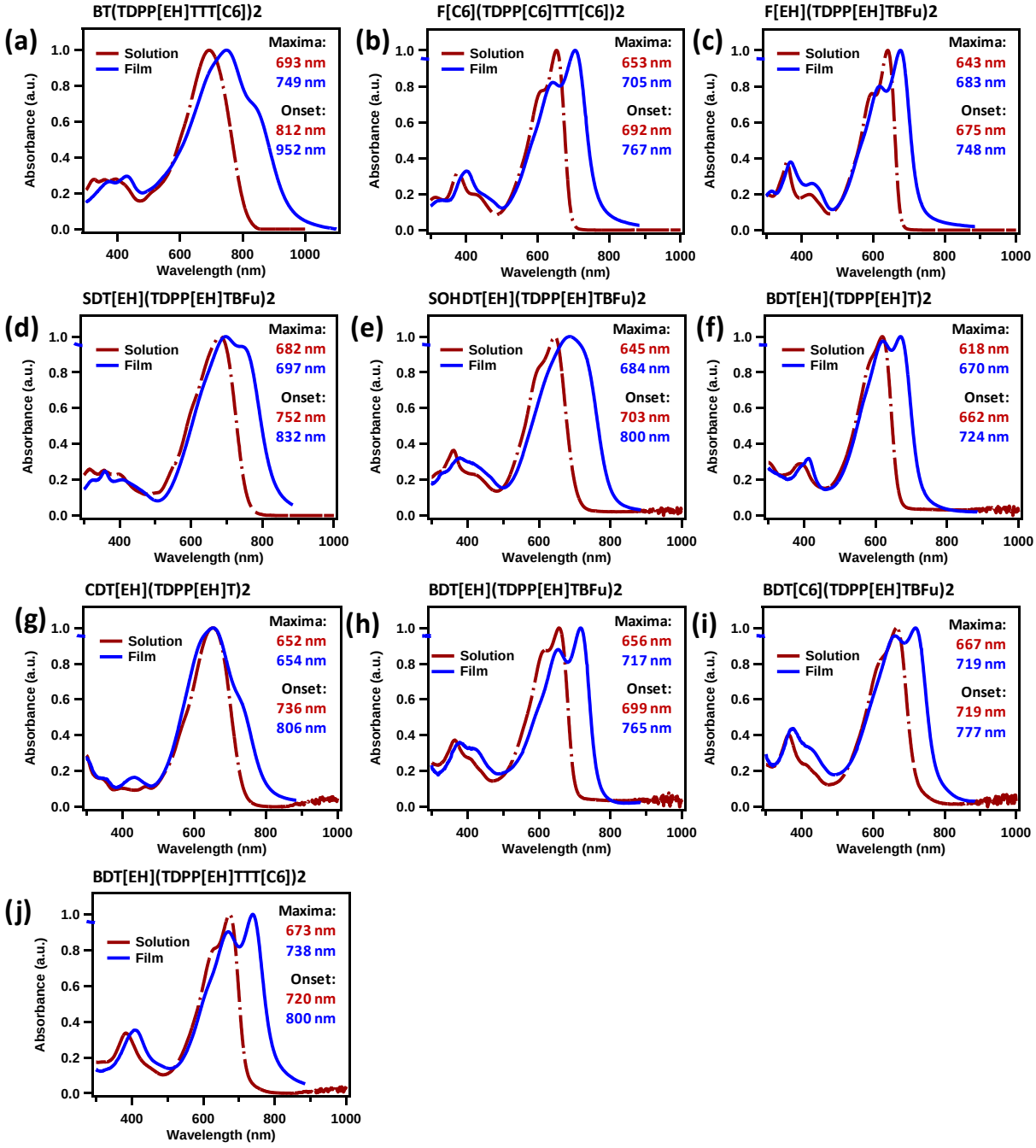

Figure S2. UV-vis absorption spectra of bis-DPP compounds. Red, dashed curves represent solution spectra while solid blue curves represent pristine films of each material. a) $BT(TDPP_{EH}TTT_{C6})_2$, b) $F_{C6}(TDPP_{C6}TTT_{C6})_2$, c) $F_{EH}(TDPP_{EH}TBFu)_2$, d) $SDT_{EH}(TDPP_{EH}TBFu)_2$, e) $SOHDT_{EH}(TDPP_{EH}TBFu)_2$ f) $BDT_{EH}(TDPP_{EH}T)_2$, g) $CDT_{EH}(TDPP_{EH}T)_2$, h) $BDT_{EH}(TDPP_{EH}TBFu)_2$, i) $BDT_{C6}(TDPP_{EH}TBFu)_2$, and j) $BDT_{C6}(TDPP_{EH}TTT_{C6})_2$.

2.2 Ultraviolet Photoelectron Spectroscopy

In order to determine HOMO energy levels, UPS spectra were obtained from films of each compound. **Figure S3** shows the UPS spectra taken for all DPP-based small molecules used in this work. In the left hand side of **Figure S3**, the high binding energy cutoff from spectra is E_{cutoff}, which is determined by linear extrapolation to zero at the yield of secondary electrons. The right side of **Figure S3** shows the HOMO region. The E_{HOMO} is the onset relative to the Fermi level (E_F) of Au (at 0 eV), where the E_F was determined from the Au substrate. From **Figure S3**, the ionization potential (IP, HOMO) is determined by using the incident photon energy ($h\nu$ =21.2 eV) for He I, E_{cutoff}, and E_{HOMO} according to the equation, IP = $h\nu$ – (E_{cutoff} - E_{HOMO}).

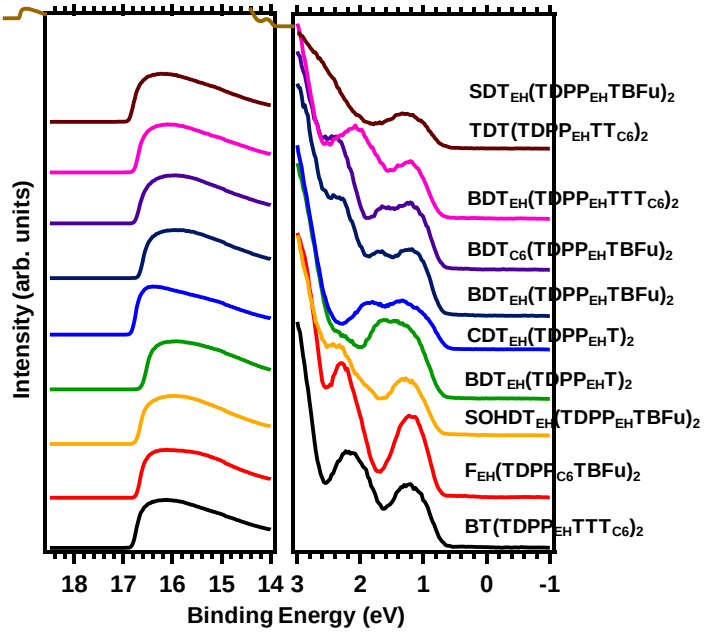

Figure S3. UPS spectra of bis-DPP compounds.

3. Current voltage characteristics of bis-DPP compounds

BHJ solar cells were prepared using blends of each bis-DPP material with $PC_{71}BM$. For each material, 3 blend ratios were prepared (30:70, 50:50 and 70:30) by spin-casting at different spin-rates; additionally, devices were thermally annealed at various temperatures. For each material, at least one solvent additive such as 1,8-octanedithiol (ODT), 1,4-diiodobutane (DIB), 1,8-diiodooctane (DIO), diiodomethane (DIM), chloronaphthalene (CN) or 1,1,2,2-

tetrabromoethane (EtBr4) were evaluated with each material. Current voltage (J-V) characteristics for each set of conditions are reported in **Figures S4-13**, the characteristics of each material are reported in tables S1-S10, compared in **Table S1** and briefly discussed in the following sections.

3.1. $BT(TDPP_{EH}TTT_{C6})_2$

In an attempt to create a material with a low band gap, we synthesized a bis-DPP material with a benzothiadiazole core unit, a strong electron withdrawing moiety which has successfully been incorporated in many polymers and small molecules with low band gaps. The current density vs. voltage (J-V) curves and external quantum efficiency (EQE) are reported in **Figure S4** and the device perameters are reported in **Table S1**. The photocurrent onset of this material occurs at 900 nm (**Figure S4**k), corresponding to a band gap of 1.38 eV. Although photocurrent generation occurs over a broad range, the quantum efficiency decreases dramatically at longer wavelengths. Despite having a low band gap, the material does not produce a very large J_{SC}, regardless of the blend ratio (**Figure S4**a, d, g). A maximum J_{SC} of ~2.2 mA/cm^2 is observed for the 50:50 ratio. Despite the low current, this system does exhibit a relatively high FF, producing a maximum of 69.8% for the 30:70 blend. Thermal annealing of all blend ratios leads to a decrease in FF and J_{SC} along with an increase in V_{OC}. Comparing the V_{OC} to the bandgap indicates that 850 mV of potential are lost in this system. Including the solvent additives ODT and DIB in 2% concentration (**Figure S4**j) leads to a considerable increase in J_{SC}, reaching up to 5.85 mA/cm^2 for DIB. Optimal performance in this system was obtained with this additive including a V_{OC} of 482 mV, a FF of 56.5% and power conversion efficiency (PCE) of 1.59%.

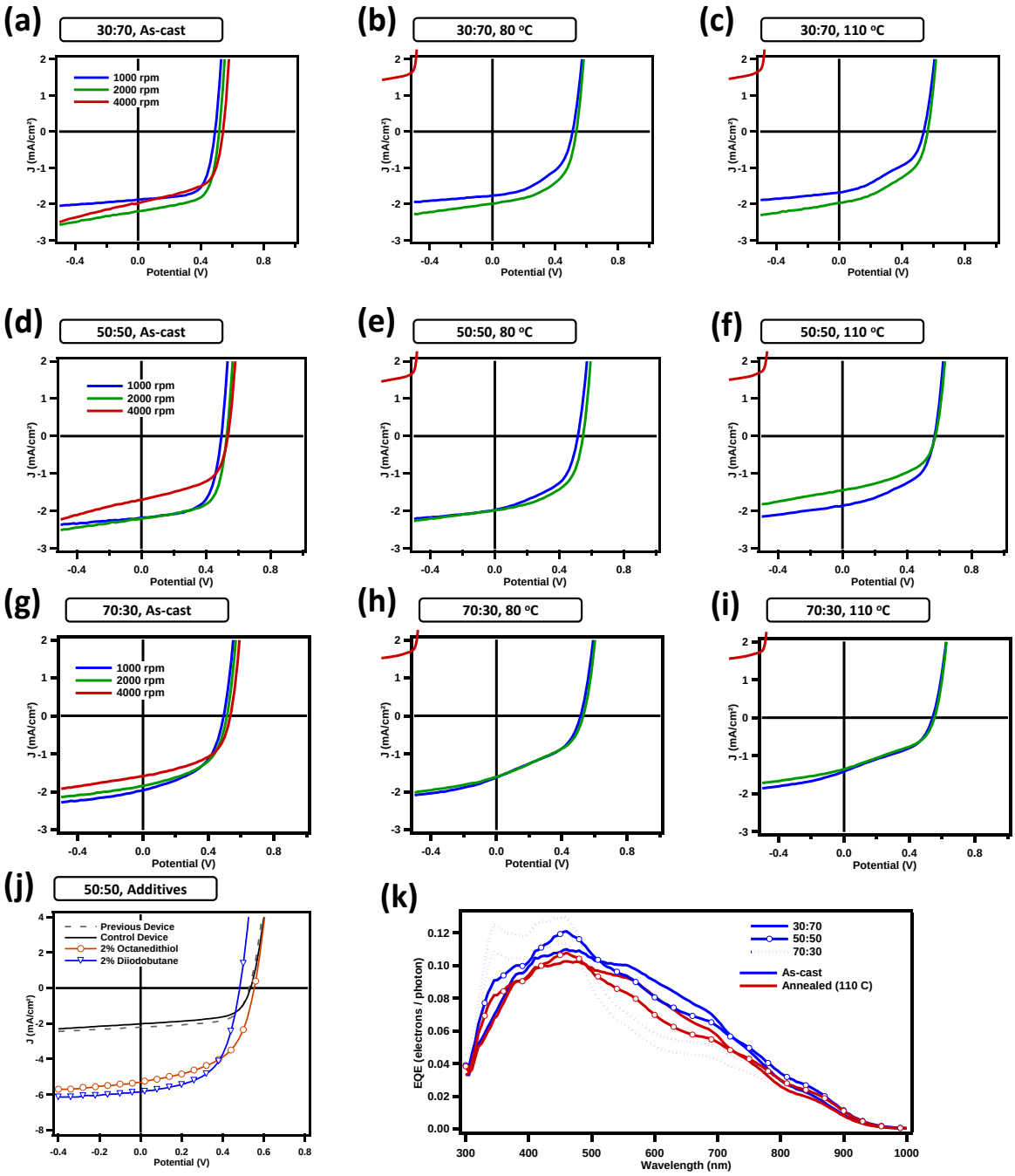

Figure S4. Solar cell characteristics of devices with a)-c) 30:70, d)-f), j) 50:50 and g)-i) 70:30 BT(TDPP$_{EH}$TTT$_{C6}$)$_2$:PC$_{71}$BM ratios. Plots a), d), g), j) show as-cast devices, b), e), h) show devices annealed at 80 ^{o}C and c), f), i) show devices annealed at 110 ^{o}C. Plot j) shows J-V characteristics of films prepared using solvent additives and the external quantum efficiency of devices with different blend ratios are plotted in k) before and after annealing at 110 ^{o}C.

Table S1. BT(TDPP$_{EH}$TTT$_{C6}$)$_2$:PC$_{71}$BM devices.

	Annealing Temp. (°C)	As-cast			80°C			110°C		
Ratio	Spin rate (rpm)	1K	2K	4K	1K	2K	4K	1K	2K	4K
30:70	J_{SC} [mA/cm^2]	1.880	2.198	1.977	1.763	1.990	1.833	1.680	1.964	1.697
	V_{OC} [V]	0.469	0.482	0.538	0.489	0.506	0.521	0.500	0.556	0.574
	FF	0.698	0.689	0.582	0.500	0.562	0.547	0.448	0.465	0.467
	PCE [%]	0.616	0.730	0.619	0.431	0.565	0.522	0.377	0.508	0.455
50:50	J_{SC} [mA/cm^2]	2.183	2.203	1.696	1.969	1.983	1.626	1.736	1.864	1.444
	V_{OC} [V]	0.464	0.511	0.504	0.486	0.534	0.526	0.504	0.549	0.544
	FF	0.670	0.655	0.569	0.521	0.538	0.527	0.498	0.494	0.495
	PCE [%]	0.679	0.738	0.486	0.498	0.569	0.451	0.436	0.505	0.389
70:30	J_{SC} [mA/cm^2]	1.956	1.844	1.586	1.625	1.609	1.383	1.410	1.355	1.229
	V_{OC} [V]	0.466	0.487	0.506	0.485	0.509	0.531	0.539	0.527	0.546
	FF	0.522	0.533	0.538	0.443	0.424	0.452	0.421	0.427	0.466
	PCE [%]	0.476	0.479	0.431	0.349	0.347	0.332	0.320	0.305	0.313

		Previous	Control	2% ODT	2% DIB
50:50	J_{SC} [mA/cm^2]	2.203	2.016	5.308	5.851
	V_{OC} [V]	0.529	0.535	0.553	0.482
	FF	0.634	0.612	0.531	0.565
	PCE [%]	0.738	0.660	1.559	1.593

3.2. $F_{C6}(TDPP_{C6}TTT_{C6})_2$

A material with bis-n-hexyl fluorene core and terthiophene end-groups was synthesized. *J-V* characteristics and EQE are plotted in **Figure S5** while the device parameters are summarized in **Table S2**. In this case, the observed photocurrent onset and onset extrapolated from DFT calculations are very close at ~760 nm. Comparing different blend ratios reveals that the largest current and best performance are obtained with a large fullerene content (30:70 ratio). Thermal annealing leads to a decrease in V_{OC} for all blend ratios. Additionally, a decrease in J_{SC} and performance occur for the fullerene rich blend (30:70) at annealing temperartures above 60 ^{o}C, while an increase in J_{SC} and performance occur at 80 ^{o}C for the blend with high donor content (70:30). The solvent additive ODT at 2% concentration was found to drastically reduce all device parameters. Optimal processing conditions for this system were found to be a 30:70

ratio, spincast at 2000 rpm and thermally annealed at 60 °C, leading to a J_{SC} of 6.2 mA/cm^2, a V_{OC} of 780 mV, a FF of 52% and a PCE of 2.5%.

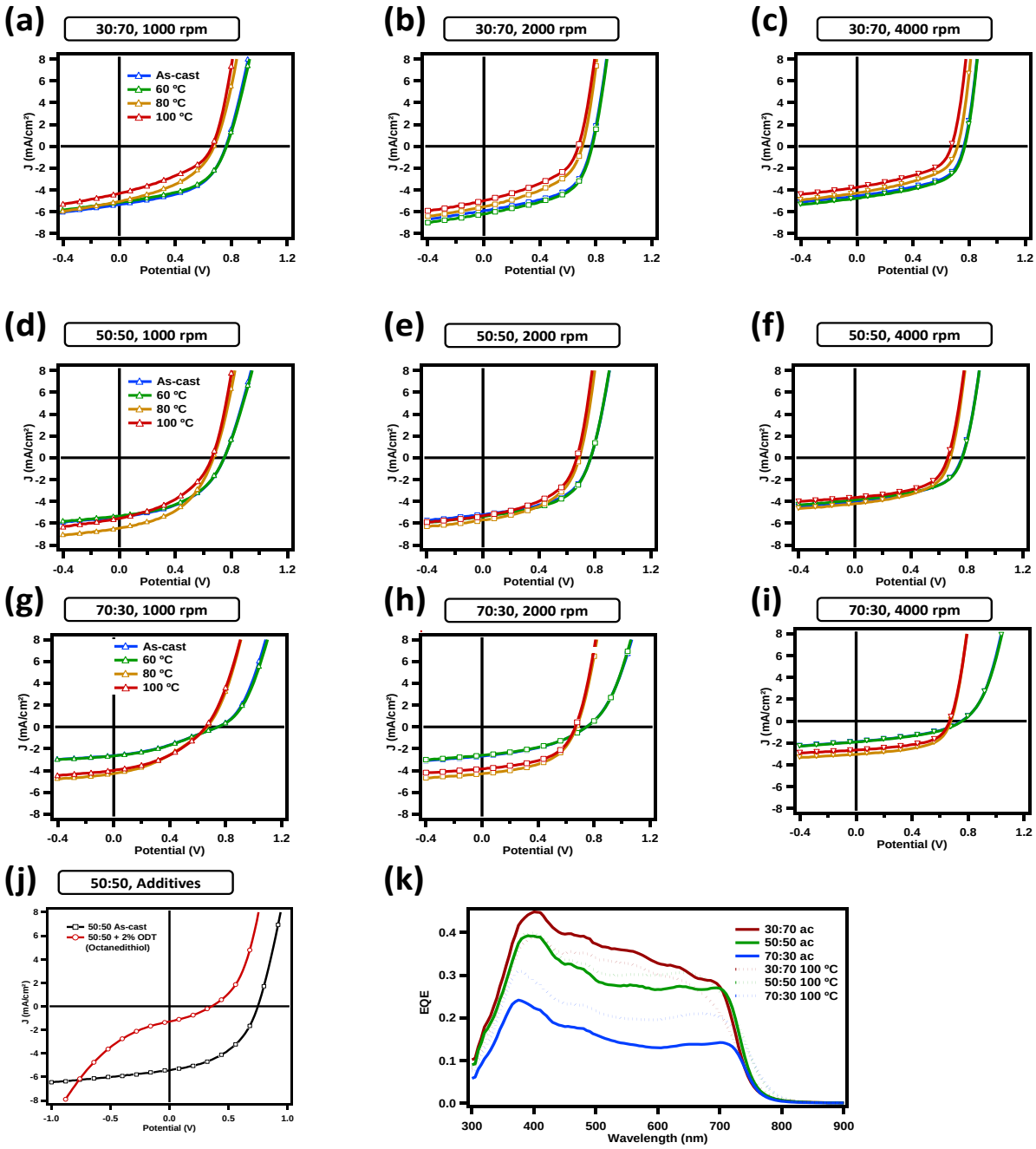

Figure S5. Solar cell characteristics of devices with a)-c) 30:70, d)-f), j) 50:50 and g)-i) 70:30 *F_{C6}(TDPP$_{C6}$TTT$_{C6}$)$_2$:PC$_{71}$BM* ratios. Plots a), d), g) show devices spin-cast at 1000 rpm, b), e), h), j) show devices spin-cast at 2000 rpm and c), f), i) show devices spin-cast at 4000 rpm. Plot j) shows J-V characteristics of films prepared using ODT and the external quantum efficiency of devices with different blend ratios are plotted in k) before and after annealing at 100 °C.

Table S2. $F_{C6}(TDPP_{EH}TTT)_2$:$PC_{71}BM$ devices.

	Spin rate (rpm)			1K				2K				4K	
Ratio	Annealing Temp. (°C)	As-cast	60°C	80°C	110°C	As-cast	60°C	80°C	110°C	As-cast	60°C	80°C	110°C
30:70	J_{SC} [mA/cm^2]	5.356	5.153	5.055	4.323	5.895	6.202	5.536	4.995	4.544	4.773	4.290	3.764
	V_{OC} [V]	0.78	0.78	0.68	0.68	0.78	0.78	0.72	0.68	0.78	0.78	0.72	0.68
	FF	0.486	0.489	0.413	0.371	0.522	0.518	0.432	0.415	0.514	0.515	0.460	0.446
	PCE [%]	2.03	1.97	1.42	1.09	2.40	2.51	1.72	1.41	1.82	1.92	1.42	1.14
50:50	J_{SC} [mA/cm^2]	5.432	5.356	6.462	5.555	5.223	5.407	5.681	5.319	3.993	3.873	4.208	3.652
	V_{OC} [V]	0.76	0.76	0.68	0.68	0.78	0.78	0.70	0.68	0.78	0.78	0.70	0.68
	FF	0.451	0.454	0.451	0.406	0.500	0.500	0.472	0.460	0.486	0.502	0.490	0.511
	PCE [%]	1.86	1.85	1.98	1.53	2.04	2.11	1.88	1.66	1.51	1.52	1.44	1.27
70:30	J_{SC} [mA/cm^2]	2.632	2.656	4.291	3.999	2.679	2.593	4.299	3.848	1.887	1.911	3.036	2.640
	V_{OC} [V]	0.76	0.76	0.68	0.66	0.76	0.76	0.68	0.68	0.76	0.76	0.68	0.68
	FF	0.332	0.333	0.353	0.391	0.388	0.393	0.495	0.501	0.394	0.401	0.541	0.535
	PCE [%]	0.66	0.67	1.03	1.03	0.79	0.77	1.45	1.31	0.57	0.58	1.12	0.96

3.3. $F_{EH}(TDPP_{EH}TBFu)_2$

A material with bis-2-ethylhexyl fluorene core and benzofuran end-groups was synthesized. *J-V* characteristics and EQE are plotted in **Figure S6** while the device parameters are summarized in **Table S3**. In this case, the observed photocurrent onset (730 nm) is slightly blue-shifted compared to the value extrapolated from DFT calculations (760 nm). Similar to the $BT(TDPP_{EH}TTT_{C6})_2$ material, the J_{SC} produced by this material is rather low considering that the band gap is fairly narrow (1.7 eV). In this case, the 50:50 ratio was found to yield the most favorable characteristics. The most significant effect that thermal annealing has for this material is to increase the FF. Using ODT as a solvent additive is found to increase the J_{SC} while decreasing the V_{OC}. An ODT concentration of 0.5% was found to be optimal for this system, leading to a J_{SC} of 4.4 mA/cm^2, a V_{OC} of 658 mV, a FF of 39% and a PCE of 1.1%.

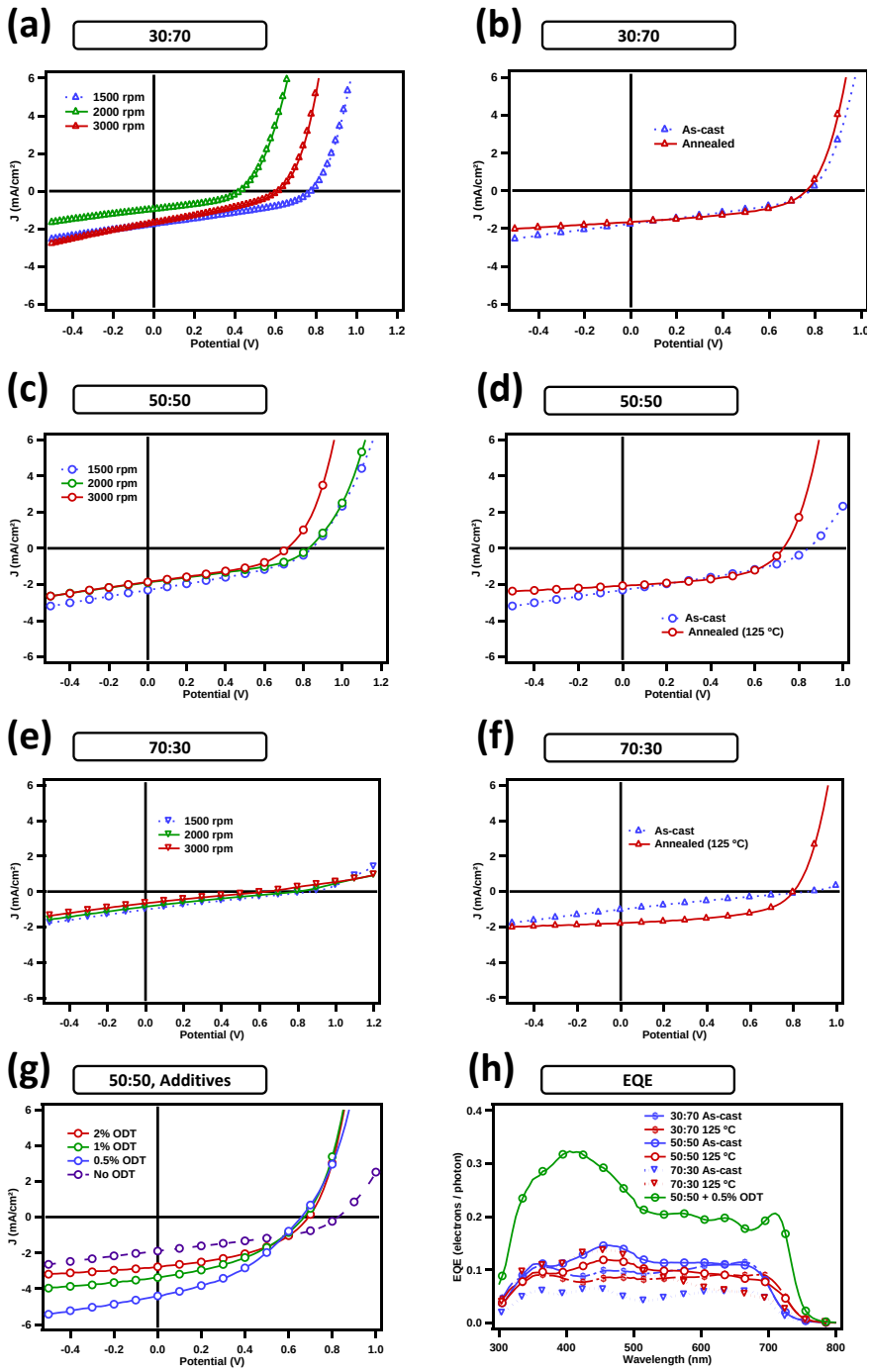

Figure S6. Solar cell characteristics of devices with a),b) 30:70, c),d) 50:50 and e),f) 70:30 $F_{EH}(TDPP_{EH}TBFu)_2$:$PC_{71}BM$ ratios. Plots a),c),e) show devices spin-cast at different spin rates, while b),d),f) show devices before and after annealing at 125 ^{o}C. Plot g) shows J−characteristics of films prepared using ODT. The EQE of devices with different blend ratios before and after annealing at 125 ^{o}C as well as 0.5% ODT are plotted in h).

Table S3. $F_{EH}(TDPP_{EH}TBFu)_2$:$PC_{71}BM$ devices.

Annealing Temp. (°C)		As-cast			Annealed (125 °C)
	Spin rate (rpm)	1.5K	2K	3K	1.5K
30:70	J_{SC} [mA/cm^2]	1.759	0.956	1.675	1.662
	V_{OC} [V]	0.779	0.428	0.615	0.761
	FF	0.364	0.396	0.328	0.460
	PCE [%]	0.499	0.162	0.338	0.582
50:50	J_{SC} [mA/cm^2]	2.313	1.896	1.857	2.070
	V_{OC} [V]	0.843	0.827	0.717	0.729
	FF	0.364	0.388	0.407	0.510
	PCE [%]	0.710	0.609	0.541	0.770
70:30	J_{SC} [mA/cm^2]	1.014	0.851	0.659	1.786
	V_{OC} [V]	0.872	0.794	0.636	0.801
	FF	0.233	0.231	0.233	0.509
	PCE [%]	0.206	0.156	0.098	0.728
50:50	Additive	0%	0.5%	1%	2%
	J_{SC} [mA/cm^2]	1.896	4.407	3.380	2.781
	V_{OC} [V]	0.827	0.658	0.671	0.691
	FF	0.388	0.392	0.401	0.441
	PCE [%]	0.609	1.138	0.910	0.846

4.4. $SDT_{EH}(TDPP_{EH}TBFu)_2$

A material with a dithienosilole core and benzofuran end-capping groups was syntheszied and devices were prepared. Photovoltaic characteristics are plotted in **Figure S7** while device properties are summarieze in **Table S4**. Predictions based on DFT calculations indicate that this material should have a narrower bandgap compared to the material without end-capping groups with a predicted photocurrent onset of about 865 nm. Thermal annealing has little effect on this material, while solvent additives allow for improvement in current density and FF. Optimal conditions for this material were found to include a 50:50 blend ratio with 0.5% DIO, yielding a J_{SC} of 9.3 mA/cm^2, a V_{OC} of 620 mV, a FF of 59% and a PCE of 3.4%.

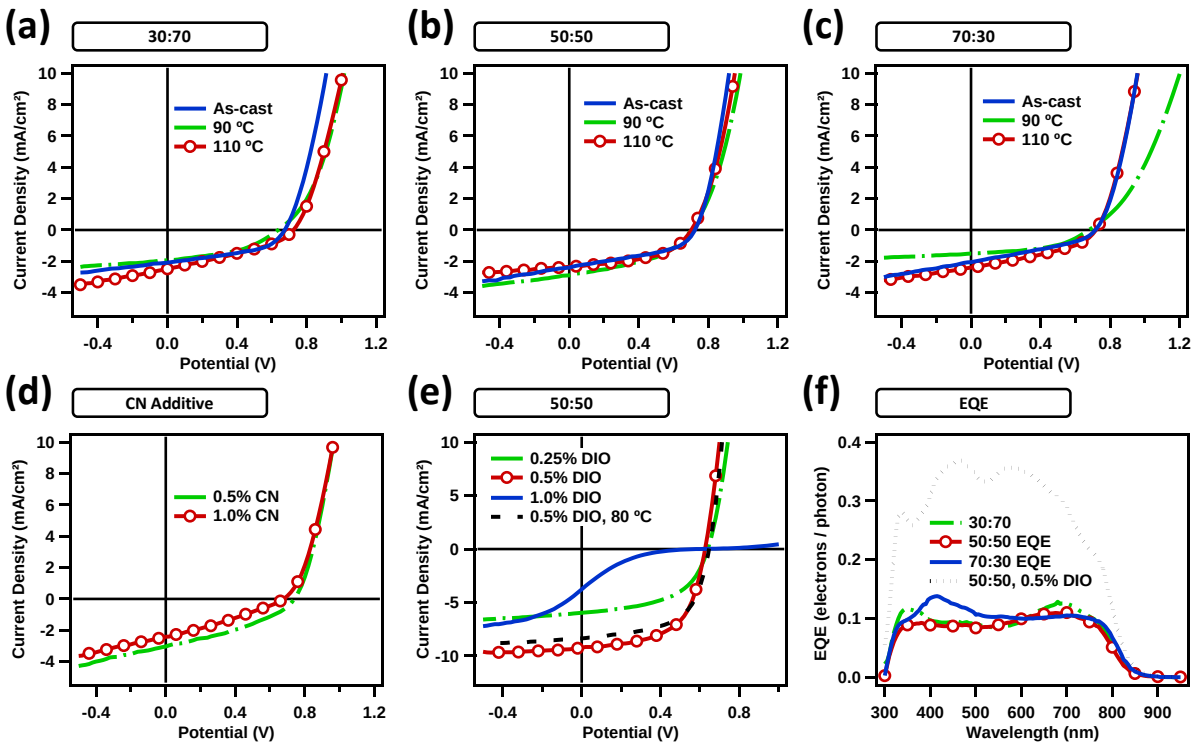

Figure S7. Solar cell characteristics of devices with a) 30:70, b) 50:50 and c) 70:30 $SDT_{EH}(TDPP_{EH}TBFu)_2$:$PC_{71}BM$ ratios annealed at different temperatures. Plots d) and e) show devices prepared with different amounts of the solvent additives CN and DIO, respectively. The EQE of devices with different blend ratios before and with 0.5% DIO are plotted in f).

Table S4. $SDT_{EH}(TDPP_{EH}TBFu)_2$:$PC_{71}BM$ devices.

	Annealing Temp. (°C)	As-cast	90 °C	110 °C
30:70	J_{SC} [mA/cm^2]	1.86	1.85	1.55
	V_{OC} [V]	0.685	0.650	0.680
	FF	0.500	0.439	0.469
	PCE [%]	0.63	0.53	0.49
50:50	J_{SC} [mA/cm^2]	2.21	2.88	2.33
	V_{OC} [V]	0.718	0.670	0.660
	FF	0.437	0.380	0.421
	PCE [%]	0.69	0.74	0.66

70:30	J_{SC} [mA/cm^2]	1.77	1.52	2.55
	V_{OC} [V]	0.723	0.680	0.720
	FF	0.332	0.471	0.357
	PCE [%]	0.42	0.49	0.65

	Additive	0.5% CN	1% CN	0.25% DIO	0.5%DIO	1% DIO
50:50	J_{SC} [mA/cm^2]	2.29	2.94	6.00	9.23	4.18
	V_{OC} [V]	0.700	0.740	0.640	0.620	0.605
	FF	0.259	0.335	0.532	0.579	0.104
	PCE [%]	0.42	0.73	2.04	3.31	0.26

3.5. SOHDT$_{EH}$(TDPP$_{EH}$TBFu)$_2$

Out of all the materials investigated, one with a 3''-(bis(2-ethylhexyl)silanolyl)-2,2':5',2'':5'',2'''-quaterthiophene core and benzofuran end-groups yields the best properties for a BHJ donor material. The preliminary J-V characteristics and EQE are plotted in **Figure S8** while the device parameters are summarized in **Table S5**. Although extrapolations based on DFT calculations predict a photocurrent onset of 890 nm, the observed photocurrent onset occured at a significantly shorter wavelength of 800 nm. Although the absorption is not as broad as predicted, the V_{OC} is found to be larger than expected, resulting in a material with a low bandgap and high V_{OC}. Becuase this material exhibited the most promising characteristics out of all materials explored in this study, a larger number of additives and processing conditions were explored in the initial screening of this compound, compared to other compounds. A detailed account of the optimization of this material can be found in the main text.

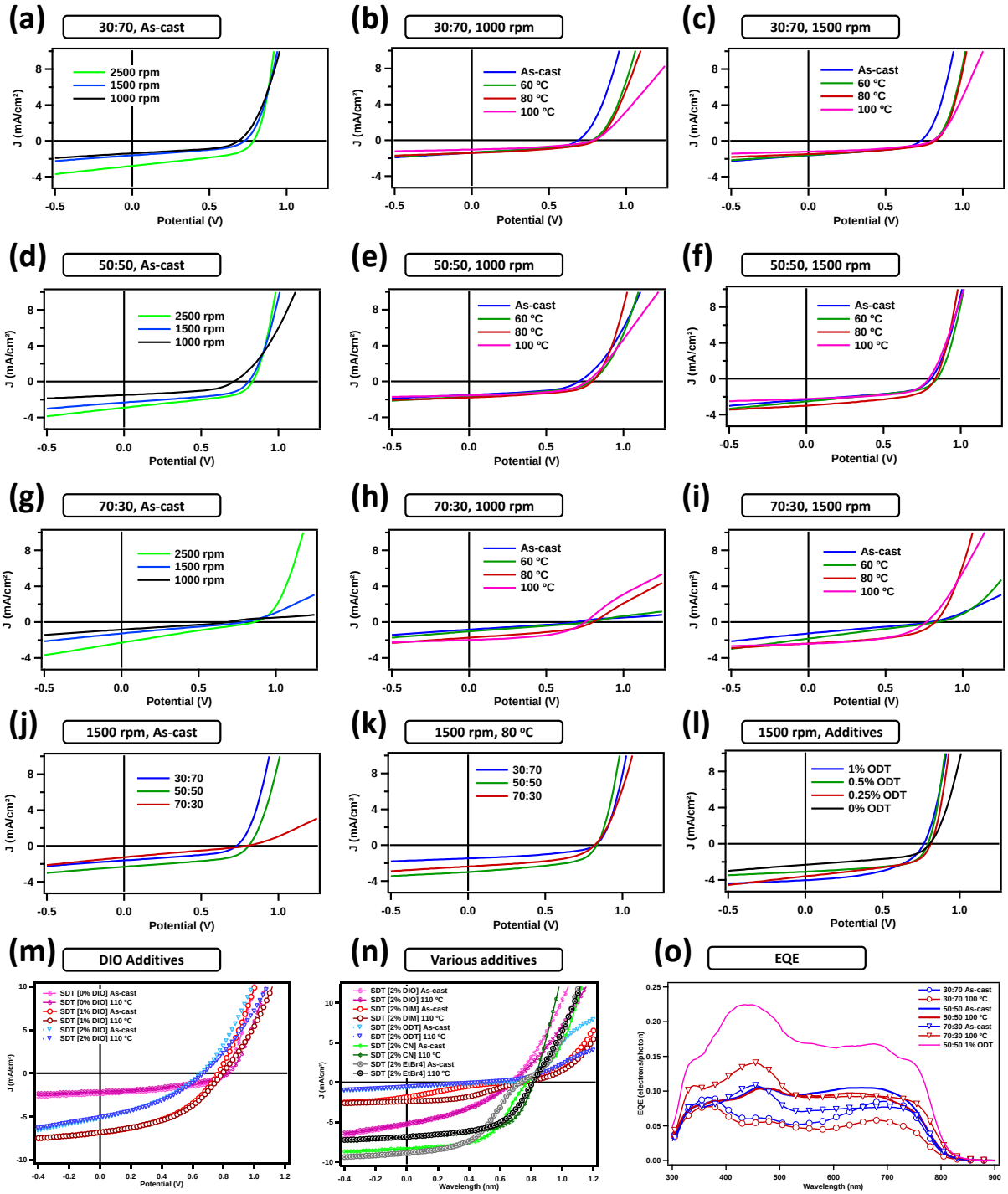

Figure S8. Solar cell characteristics of devices with a)-c) 30:70, d)-f),j) 50:50 and g)-i) 70:30 *SOHDT$_{EH}$(TDPP$_{EH}$TBFu)$_2$:PC$_{71}$BM* ratios. Plots a),d),g) show devices spincast at different spinrates, b),e),h) show devices spincast at 1000 rpm and annealed at various temperatures, c),f),i) show devices spincast at 1500 rpm and annealed at various temperatures. Plots j),k) compare J-V characteristics of films with different blend ratios, plots l) and m) compare J-V characteristics of films with varying amounts of ODT and DIO, respectively. Plot n) compares the J-V characteristics of films with various additives and the EQE of devices are plotted in o).

Table S5. $SOHDT_{EH}(TDPP_{EH}TBFu)_2$:$PC_{71}BM$ devices.

	Annealing Temp. (°C)	As-cast			60°C		80°C		100°C	
	Spin rate (rpm)	2.5K	1.5K	1K	1.5K	1K	1.5K	1 K	1.5K	1 K
30:70	J_{SC} [mA/cm^2]	2.799	1.613	1.389	1.593	1.357	1.472	1.416	1.199	1.035
	V_{OC} [V]	0.785	0.728	0.688	0.806	0.779	0.823	0.801	0.802	0.785
	FF	0.447	0.429	0.461	0.379	0.392	0.424	0.427	0.438	0.428
	PCE [%]	0.982	0.504	0.440	0.486	0.415	0.514	0.484	0.421	0.347
50:50	J_{SC} [mA/cm^2]	2.910	2.329	1.494	2.536	1.681	3.004	1.795	2.259	1.548
	V_{OC} [V]	0.832	0.807	0.712	0.846	0.787	0.835	0.799	0.793	0.766
	FF	0.452	0.488	0.481	0.435	0.431	0.510	0.490	0.553	0.518
	PCE [%]	1.093	0.917	0.512	0.933	0.570	1.278	0.703	0.990	0.614
70:30	J_{SC} [mA/cm^2]	2.310	1.264	0.835	1.847	1.043	2.391	1.729	2.420	1.987
	V_{OC} [V]	0.860	0.792	0.685	0.834	0.777	0.820	0.801	0.763	0.752
	FF	0.244	0.262	0.286	0.252	0.264	0.477	0.411	0.484	0.488
	PCE [%]	0.485	0.262	0.164	0.388	0.214	0.936	0.569	0.894	0.730

		1% ODT	0.5% ODT	0.25% ODT
50:50	J_{SC} [mA/cm^2]	4.038	3.107	3.598
	V_{OC} [V]	0.768	0.795	0.813
	FF	0.491	0.588	0.494
	PCE [%]	1.522	1.452	1.446

	DIO	0%, As-cast	0%, 110°C	1%, As-cast	1%, 110°C	2%, As-cast	2%, 110°C
50:50	J_{SC} [mA/cm^2]	2.327	2.132	6.854	6.813	5.253	5.167
	V_{OC} [V]	0.805	0.831	0.765	0.793	0.666	0.679
	FF	0.472	0.397	0.439	0.443	0.359	0.370
	PCE [%]	0.885	0.702	2.306	2.392	1.255	1.298

	Additive	2% DIM, As-cast	2% DIM, 110°C	2% ODT, As-cast	1%, 110°C	2%, As-cast	2%, 110°C
50:50	J_{SC} [mA/cm^2]	1.849	2.386	0.707	6.813	5.253	5.167
	V_{OC} [V]	0.644	0.745	0.700	0.793	0.666	0.679
	FF	0.204	0.402	0.205	0.443	0.359	0.370
	PCE [%]	0.243	0.715	0.102	2.392	1.255	1.298

3.6. $BDT_{EH}(TDPP_{EH}T)_2$

Due to the synthetic difficulty of end-capping bis-DPP type molecules, we sought to compare the properties of molcules with terminal, unsubstituted thiophene groups to other end-capping groups. A material with 4,8-bis-(2-ethylhexyoxy)benzo(1,2-*b*:4,5-*b*′)dithiophene core was synthesized with no end-capping groups. J-V characteristics and EQE are plotted in **Figure S9** while the device parameters are summarized in **Table S5**. The observed photocurrent onset (730 nm) matches the value extrapolated from DFT calculations. Comparing the band gap (1.7 eV) to the largest observed V_{OC} indicates that at least 845 mV of potential are lost during electron transfer and charge collection for this system. As-cast films of this material produce the largest J_{SC} when the acceptor content is high (30:70 ratio), yielding a J_{SC} of 7.4 mA/cm^2. Thermal annealing at 100 ^{o}C is found to degrade all parameters of the 30:70 blend, while improving the performance of the 50:50 blend and dramatically increasing the J_{SC} of the 70:30 blend. The 50:50 blend annealed at 100 ^{o}C was found to be optimal for this system, leading to a J_{SC} of 8.3 mA/cm^2, a V_{OC} of 775 mV, a FF of 44% and a PCE of 2.8%. Solvent addtives (DIO and CN) were not found to provide any benefit for this system.

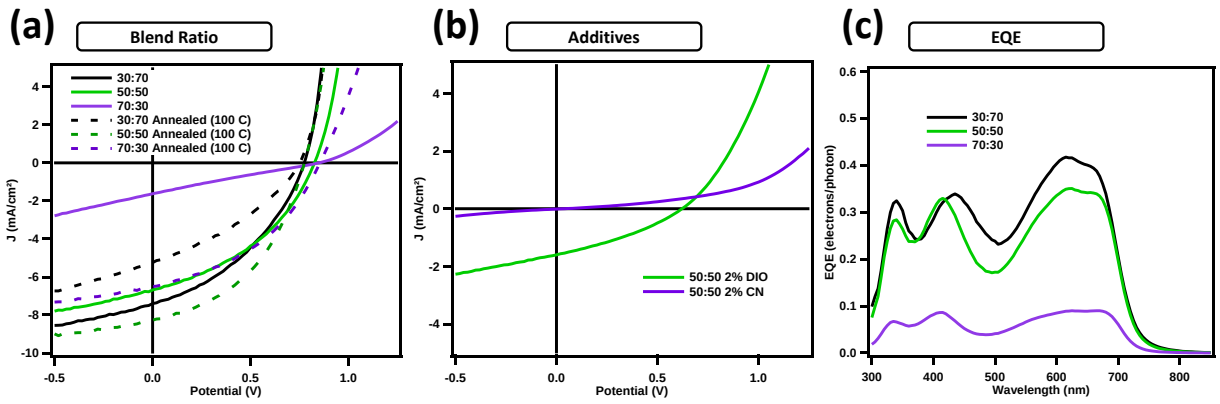

Figure S9. Solar cell characteristics of *$BDT_{EH}(TDPP_{EH}T)_2$:$PC_{71}BM$* devices. Comparison of J-V characteristics of 30:70, 50:50 and 70:30 blend ratios a), solvent additives b) and EQE spectra c).

Table S6. $BDT_{EH}(TDPP_{EH}T)_2$:$PC_{71}BM$ devices.

	30:70		50:50		70:30	
	As-cast	Annealed	As-cast	Annealed	As-cast	Annealed
J_{SC} [mA/cm^2]	7.397	5.253	6.679	8.266	1.622	6.503
V_{OC} [V]	0.774	0.750	0.826	0.775	0.847	0.855
FF	0.394	0.349	0.401	0.444	0.235	0.413
PCE [%]	2.258	1.376	2.210	2.846	0.323	2.298

	50:50, 2% CN	50:50, 2% DIO
J_{SC} [mA/cm^2]	0.010	1.597
V_{OC} [V]	0.029	0.622
FF	0.212	0.328
PCE [%]	0.000	0.326

3.7. $CDT_{C12}(TDPP_{EH}T)_2$

A material with bis-4,4(2-ethylhexyl) cyclopentadithiophene core was synthesized with no end-capping groups. J-V characteristics and EQE are plotted in **Figure S10** while the device parameters are summarized in **Table S7**. The observed photocurrent onset (730 nm) matches the value extrapolated from DFT calculations. Comparing the band gap (1.7 eV) to the largest observed V_{OC} indicates that at least 845 mV of potential are lost during electron transfer and charge collection for this system. As-cast films of this material produce the largest J_{SC} when the acceptor content is high (30:70 ratio), yielding a J_{SC} of 7.4 mA/cm^2. Thermal annealing at 100 ^oC is found to degrade all parameters of the 30:70 blend, while improving the performance of the 50:50 blend and dramatically increasing the J_{SC} of the 70:30 blend. In an attempt to increase the V_{OC}, a molybdenum trioxide interlayer was employed in the following way: a suspension of solid MoO_3 powder (Aldrich, 99.99%) in methanol was filtered through a 0.45 μm PTFE filter and the filtrate spincast atop the PEDOT:PSS layer after it had been annealed as described in the main text. The treated PEDOT:PSS was annealed again at 100 ^oC for 2 minutes prior to spincasting the active layer. X-ray photoemission spectroscopy of films prepared in this manner reveal that the element Mo is present on the PEDOT:PSS surface. Although the MoO_3 interlayer is found to improve the V_{OC}, the improvement is accompanied by a decrease in FF and in the case of the 30:70 blend, J_{SC} as well. Solvent addtives (DIO and CN) were not found to provide any benefit for this system. The as-cast 30:70 blend was found to be optimal for this system, leading to a J_{SC} of 4.4 mA/cm^2, a V_{OC} of 623 mV, a FF of 33% and a PCE of 0.90%.

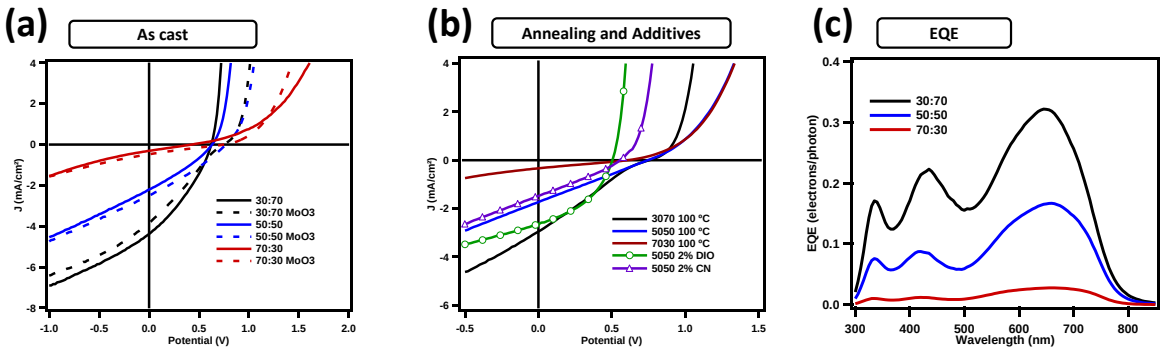

Figure S10. Solar cell characteristics of *$CDT_{C12}(TDPP_{EH}T)_2$:$PC_{71}BM$* devices. Comparison of J-V characteristics of 30:70, 50:50 and 70:30 blend ratios a), solvent additives and annealing temperatures b) and EQE spectra c).

Table S7. $CDT_{C12}(TDPP_{EH}T)_2$:$PC_{71}BM$ devices.

	30:70		50:50		70:30	
	As-cast	As-cast, MoO_3	As-cast	As-cast, MoO_3	As-cast	As-cast, MoO_3
J_{SC} [mA/cm^2]	4.377	3.832	2.196	2.491	0.304	0.475
V_{OC} [V]	0.623	0.748	0.631	0.769	0.422	0.747
FF	0.330	0.259	0.307	0.298	0.252	0.233
PCE [%]	0.899	0.741	0.426	0.570	0.032	0.082
	30:70, 110°C	50:50, 110°C	70:30, 110°C	2% DIO	2% CN	
J_{SC} [mA/cm^2]	3.832	2.491	0.475	2.650	1.484	
V_{OC} [V]	0.748	0.769	0.747	0.503	0.554	
FF	0.259	0.298	0.233	0.414	0.284	
PCE [%]	0.741	0.570	0.082	0.552	0.233	

3.8. $BDT_{EH}(TDPP_{EH}TBFu)_2$

A material with a BDT core and benzofuran end-capping groups was syntheszied and devices were prepared. Photovoltaic characteristics are plotted in **Figure S11** while device properties are summarieze in **Table S8**. Predictions based on DFT calculations indicate that this

material should have a narrower band gap compared to the material without end-capping groups (with a photocurrent onset of about 810 nm compared to 730 for the parent material) while still producing a relatively high V_{OC} of 870 mV (compared to 910 mV for the parent material). It appears that the bandgap is wider and the HOMO and LUMO of this material are not as deep as expected, as the observed phtocurrent onset occurs at 780 nm while the observed V_{OC} is not greater than 810 mV. In this case, it seems that end-capping with benzofuran degrades device properties compared to the material without end-capping. Thermal annealing is found to cause a small increase in V_{OC} and otherwise have relatively little effect, while solvent additive CN is found to increase J_{SC} while decreasing the FF of devices. A MoO_3 interlayer was employed as in the CDT material, however, it was not found to provide any benefit. Optimal conditions for this material were found to include a 50:50 blend ratio with 2% CN, yielding a J_{SC} of 6.4 mA/cm^2, a V_{OC} of 785 mV, a FF of 42% and a PCE of 2.1%.

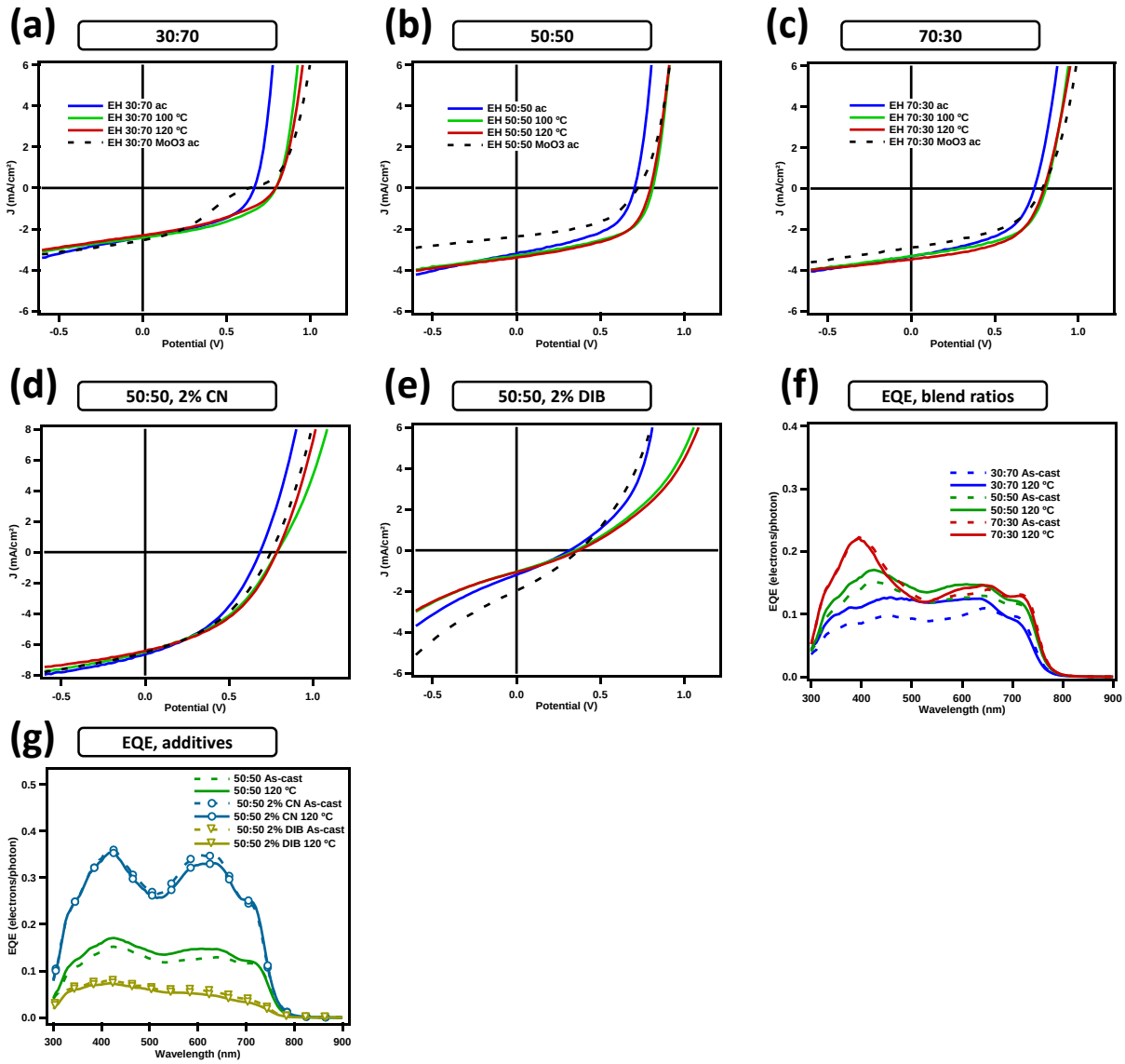

Figure S11. Solar cell characteristics of *$BDT_{EH}(TDPP_{EH}TBFu)_2$:$PC_{71}BM$* devices. Comparison of J-V characteristics of 30:70 a), 50:50 b) and 70:30 blend ratios c). J-V characteristics of devices with solvent additives CN and DIB are plotted in d) and e) respectively. EQE spectra of devices prepared at different blend ratios with and without thermal annealing are plotted in f), while EQE spectra of devices prepared with solvent additives are plotted in g).

Table S8. $BDT_{EH}(TDPP_{EH}TBFu)_2$:$PC_{71}BM$ devices.

		As-cast	100°C	120°C	A-C MoO_3
30:70	J_{SC} [mA/cm^2]	2.405	2.415	2.313	2.552
	V_{OC} [V]	0.665	0.794	0.792	0.636
	FF	0.456	0.428	0.390	0.327
	PCE [%]	0.730	0.821	0.714	0.531
50:50	J_{SC} [mA/cm^2]	3.218	3.303	3.393	2.384
	V_{OC} [V]	0.704	0.812	0.799	0.724
	FF	0.480	0.520	0.522	0.484
	PCE [%]	1.088	1.394	1.417	0.835
70:30	J_{SC} [mA/cm^2]	3.328	3.303	3.486	2.889
	V_{OC} [V]	0.737	0.806	0.795	0.784
	FF	0.483	0.520	0.525	0.469
	PCE [%]	1.185	1.383	1.456	1.061
50:50, 2% CN	J_{SC} [mA/cm^2]	6.633	6.495	6.426	6.528
	V_{OC} [V]	0.685	0.786	0.785	0.750
	FF	0.410	0.404	0.422	0.402
	PCE [%]	1.862	2.061	2.131	1.968
50:50, 2% DIB	J_{SC} [mA/cm^2]	1.192	1.040	1.062	1.979
	V_{OC} [V]	0.317	0.351	0.371	0.371
	FF	0.280	0.286	0.290	0.294
	PCE [%]	0.106	0.104	0.114	0.216

3.9. $BDT_{C6}(TDPP_{EH}TBFu)_2$

Another material with a BDT core and benzofuran end-capping groups was syntheszied and devices were prepared, however, this material comprised a BDT moiety functionalized with linear n-hexyl chains as opposed to 2-ethylhexyl. Photovoltaic characteristics are plotted in **Figure S12** while device properties are summarieze in **Table S9**. The incorporation of linear alkyl chains allows more extensive aggregation and red-shifting of absorption compared to the branched alkyl chains, as this material exhibits a photocurrent onset of 800 nm, 20 nm red-shifted compared to the 2-ethylhexyl derivative. However, the solubility of this material is rather poor compared to the ethylhexyl derivative; undissolved solids were present in the 70:30 ratio and filtered out prior to spincasting. Compared to the 2-ethylhexyl derivative, devices were found to exhibit a slightly larger J_{SC}s and slighly lower V_{OC}s. Thermal annealing was not found to have a large effect, except in the case of the high donor ratio blend (70:30), in which the J_{SC} increased considerably. Solvent additives CN and DIB were not found to provide much benefit for this system. Optimal device fabrications were found to include a 70:30 blend ratio annealed at 120 ^{o}C, yielding a J_{SC} of 6.5 mA/cm^2, a V_{OC} of 683 mV, a FF of 43% and a PCE of 1.9%.

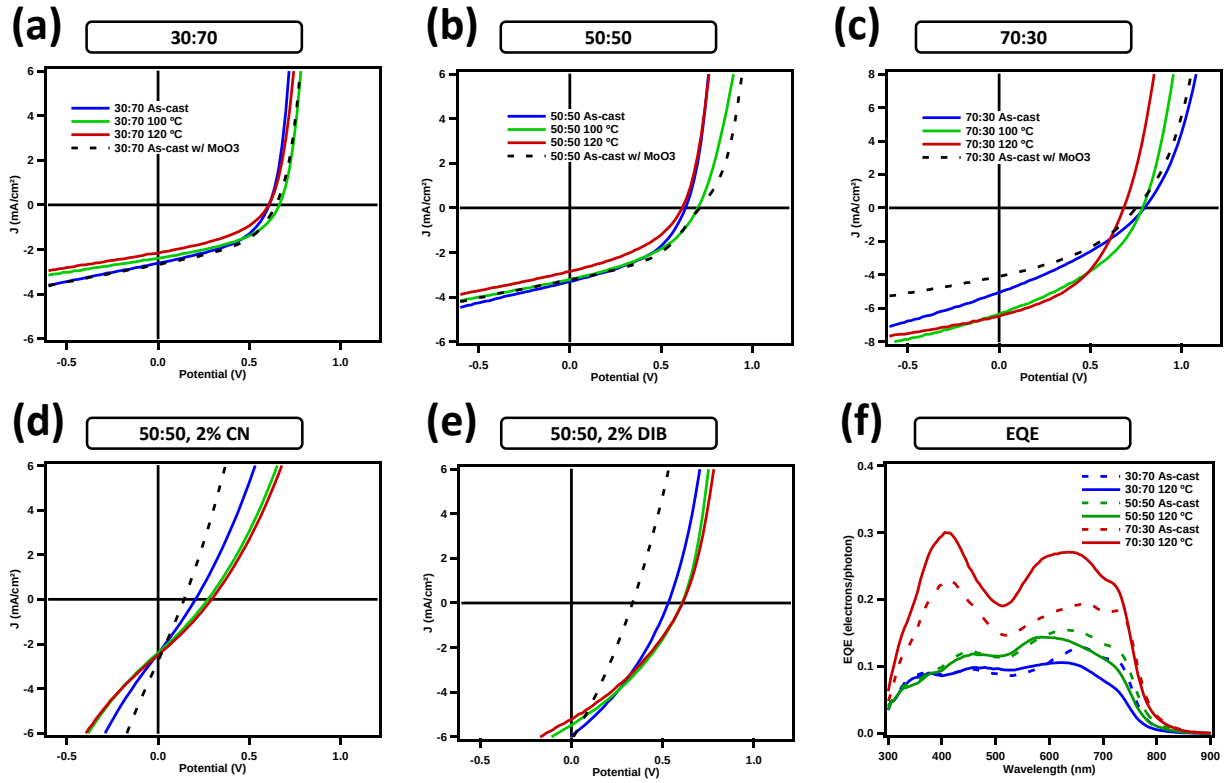

Figure S12. Solar cell characteristics of *$BDT_{C6}(TDPP_{EH}TBFu)_2$:$PC_{71}BM$* devices. Comparison of J-V characteristics of 30:70 a), 50:50 b) and 70:30 blend ratios c). J-V characteristics of

devices with solvent additives CN and DIB are plotted in d) and e) respectively. EQE spectra of devices prepared at different blend ratios with and without thermal annealing are plotted in f).

Table S9. $BDT_{C6}(TDPP_{EH}TBFu)_2$:$PC_{71}BM$ devices.

		As-cast	100°C	120°C	A-C MoO_3
30:70	J_{SC} [mA/cm^2]	2.609	2.388	2.156	2.678
	V_{OC} [V]	0.608	0.664	0.605	0.645
	FF	0.449	0.443	0.412	0.448
	PCE [%]	0.712	0.702	0.537	0.775
50:50	J_{SC} [mA/cm^2]	3.293	3.211	2.850	3.208
	V_{OC} [V]	0.634	0.701	0.615	0.712
	FF	0.436	0.412	0.393	0.440
	PCE [%]	0.909	0.928	0.690	1.005
70:30	J_{SC} [mA/cm^2]	5.059	6.339	6.481	4.105
	V_{OC} [V]	0.796	0.785	0.683	0.751
	FF	0.326	0.380	0.432	0.385
	PCE [%]	1.312	1.890	1.913	1.185
50:50, 2% CN	J_{SC} [mA/cm^2]	2.416	2.398	2.506	2.759
	V_{OC} [V]	0.204	0.273	0.293	0.142
	FF	0.267	0.278	0.279	0.258
	PCE [%]	0.132	0.182	0.205	0.102
50:50, 2% DIB	J_{SC} [mA/cm^2]	5.989	5.482	5.218	6.148
	V_{OC} [V]	0.530	0.606	0.609	0.335
	FF	0.327	0.333	0.329	0.288
	PCE [%]	1.038	1.107	1.046	0.591

3.10. $BDT_{EH}(TDPP_{EH}TTT_{C6})_2$

A third material with a BDT core and terthiophene end-capping groups was syntheszied and devices were prepared. Photovoltaic characteristics are plotted in **Figure S13** while device properties are summarieze in **Table S10**. This material shows a slightly wider band gap and slightly lower V_{OC} than values extrapolated from DFT; the observed photocurrent onset occurs at

800 nm (825 predicted) while the observed V_{OC} is up to 670 mV (720 predicted). Compared to the benzofuran end-capping group, terthiophene tends to produce a larger JSC even though the two compounds have the same photocurrent onset. CN solvent additive is found to produce the optimum conditions for this material including a J_{SC} of 10 mA/cm^2, a V_{OC} of 569 mV, a FF of 49% and a PCE of 2.8%.

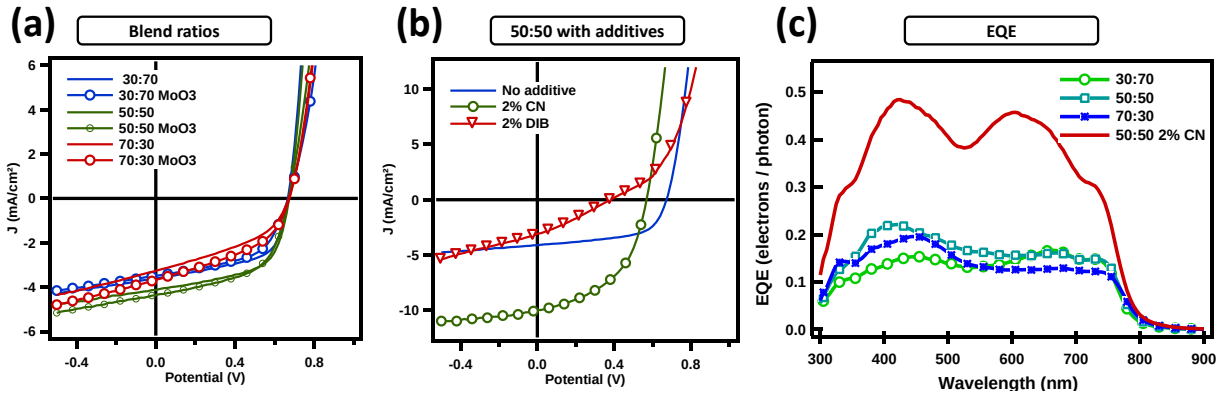

Figure S13. Solar cell characteristics of *$BDT_{EH}(TDPP_{EH}TTT_{C6})_2$:$PC_{71}BM$* devices. J-V characteristics of 30:70, 50:50 70:30 blend ratios are plotted in a), while devices prepared with solvent additives are plotted in b). EQE spectra of devices prepared at different blend ratios with and CN are plotted in c).

Table S10. $BDT_{EH}(TDPP_{EH}TTT_{C6})_2$:$PC_{71}BM$ devices.

	30:70		50:50		70:30	
	As-cast	As-cast, MoO_3	As-cast	As-cast, MoO_3	As-cast	As-cast, MoO_3
J_{SC} [mA/cm^2]	3.603	3.479	4.122	4.365	3.256	3.660
V_{OC} [V]	0.667	0.667	0.673	0.670	0.670	0.674
FF	0.578	0.538	0.583	0.549	0.416	0.433
PCE [%]	1.389	1.249	1.617	1.606	0.907	1.069

50:50	No additive	2% CN	2% DIB
J_{SC} [mA/cm^2]	4.122	10.049	3.100
V_{OC} [V]	0.673	0.569	0.380
FF	0.583	0.486	0.288
PCE [%]	1.617	2.776	0.339

Table S11. Summary.

Material	Best ratio	Solv. Additives	Ann. Effect	Solv. Add. Effect	Rs 5050
$BT(TDPP_{EH}TTT)_2$	5050	DIB, ODT	Voc↑FF,Jsc↓	Jsc↑	4.4-6.5
$F_{C6}(TDPP_{EH}TTT)_2$	3070	ODT	FF,Jsc↑Voc↓	Terrible, SS	10-16
$F_{EH}(TDPP_{EH}TBFu)_2$	5050	ODT	FF↑↑	Jsc↑Voc↓	6.6-9.5
$SOHDT_{EH}(TDPP_{EH}TBFu)_2$	5050	ODT, DIO, DIM, CN, EtBr4	Jsc, Voc, FF↑	Jsc, FF↑	7-13
$BDT_{EH}(TDPP_{EH}T)_2$	5050	CN	FF,Jsc↑ 7030	Terrible, SS	4.2ac 7.1an
$CDT_{EH}(TDPP_{EH}T)_2$	3070	DIO, CN	Nothing good	Nothing good	3.4ac 22an
$BDT_{EH}(TDPP_{EH}TBFu)_2$	7030	DIB, CN	Jsc, Voc, FF↑	Jsc↑FF↓	3.0ac, 8.5cn
$BDT_{C6}(TDPP_{EH}TBFu)_2$	7030	DIB, CN	FF,Jsc↑Voc↓	Nothing good	3.5ac, 13an
$BDT_{EH}(TDPP_{EH}TTT_{C6})_2$	5050	DIB, CN	NA	Jsc↑Voc, FF↓	2.5

3.11. Comparison of observed properties to predicted properties.

The observed bandgap, V_{OC}, HOMO and LUMO are compared to predictions based on DFT calculations for each compound and reported in **Figure S14**. Prior to synthesis, the HOMO and LUMO values of each compound were estimated from gas-phase DFT calculations using the observed shifts between the HOMO and LUMO of the **DPP(TBFu)$_2$** compound, where offsets of 0.36 and 0.65 eV for HOMO and LUMO levels were observed, respectively. Although there is some variation between predicted and observed HOMO and LUMO values, the absorption onsets predicted by the difference between predicted HOMO and LUMO values track very well with observed absorption onsets for thin films. Finally, V_{OC}s were predicted by comparing DFT calculated HOMO levels for each compound to the calculated HOMO of **DPP(TBFu)$_2$**, (that is, assuming a DFT HOMO value of 4.84 eV corresponds to an optimized V_{OC} of 0.92 V using $PC_{71}BM$ as an acceptor). The correlation between predicted and observed V_{OC} shows the poorest correlation, likely because the V_{OC} depends on device fabrication, whereas the HOMO, LUMO and bandgap can be considered intrinsic material properties. The materials $BT(TDPPTTT)_2$ and $TDT(TDPPTT)_2$ exhibit significantly lower V_{OC}s than expected and are the two data points furthest from the 1:1 correlation in Fig. S14d. $BT(TDPPTTT)_2$ has a relatively low LUMO offset with $PC_{71}BM$, which may retard electron transfer and affect the V_{OC}. It is not clear why $TDT(TDPPTT)_2$ does not produce a larger V_{OC} (observed VOC ~ 570 mV), as the observed

HOMO (5.00 eV) is close to those of SDT(TDPPTBFu)$_2$ and CDT(TDPPT)$_2$, which both produce significantly larger V_{OC}s (720 and 770 mV, respectively) using PC$_{71}$BM as an acceptor.

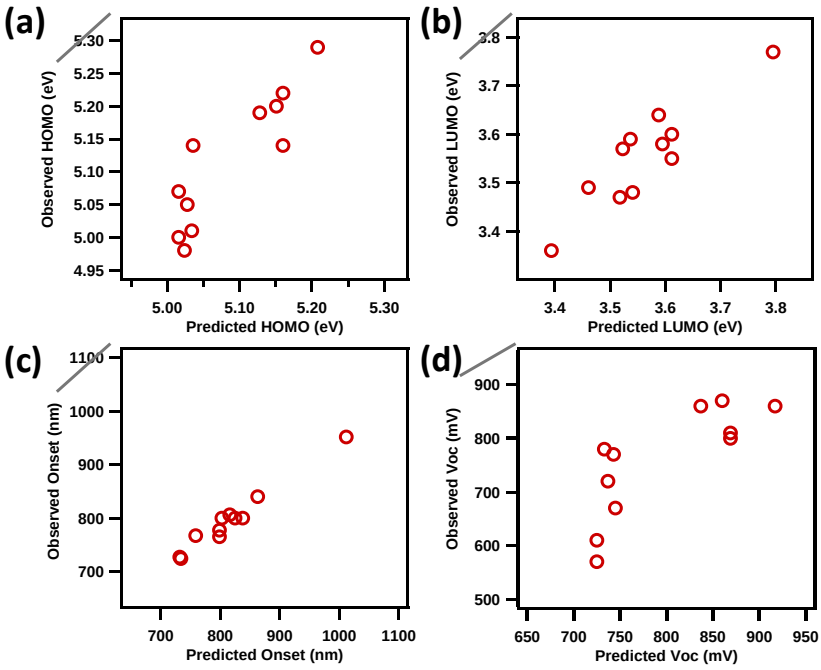

Figure S14. Comparison of predicted material properties based on DFT calculations to observed properties. a) and b) compare predicted HOMO and LUMO values to observed HOMO and LUMO values taken from UPS data and absorption onsets. HOMO and LUMO values for each compound were predicted by offsetting calculated, gas-phase DFT energy levels by the same offsets observed in DPP(TBFu)$_2$ (0.36 and 0.65 eV offsets for HOMO and LUMO levels, respectively). c) compares predicted absorption onsets based on the energy gap between predicted HOMO and LUMO values to observed absorption onsets, and d) compares predicted V$_{OC}$s based on shifts in DFT-calculated HOMO levels relative to the DFT-calculated HOMO of DPP(TBFu)$_2$ to observed V_{OC}s. Grey lines represent a 1 to 1 correlation.

4. Hole mobilities of SOHDT(TDPPTBFu)$_2$ and SOHDT(TDPPTBFu)$_2$:PC$_{71}$BM blends

Hole mobilities (μ_h)were measured by preparing hole only diodes using films of SOHDT(TDPPTBFu)$_2$ and SOHDT(TDPPTBFu)$_2$:PC$_{71}$BM and fitting the J-V curves using the space-charge limited current model. The architecture used to fabricate devices was ITO/PEDOT:PSS/test layer/Au where test layers were processed by thermal or solvent vapor annealing and had thickness' in the range of 110 to 140 nm. Current voltage characteristics of the devices are plotted in **Figure S15**.

We find that the pure material has a μ_h of 1.5×10^{-5} cm^2/Vs in the as-cast state. The mobility decreases by an order of magnitude to 1.1×10^{-6} cm^2/Vs after annealing at 100 ^{o}C for 10 minutes.

Solvent vapor annealing the pure material with 1,2-dichlorbenzene is found to have a relatively small effect, reducing μ_h to 1.2×10^{-5} cm^2/Vs.

The μ_h of the blended material with $PC_{71}BM$ is about an order of magnitude higher than the pristine μ_h at 2.5×10^{-4} cm^2/Vs. Using 0.5% CN additive is found to decrease the μ_h somewhat to 2.6×10^{-5} cm^2/Vs. After annealing the smooth film prepared with the additive at 100 ^oC or with 1,2-dichlorobenzene solvent vapor for 4 min., the mobility increases somewhat to 5.1 or 6.6 $\times$ 10^{-5} cm^2/Vs, respectively.

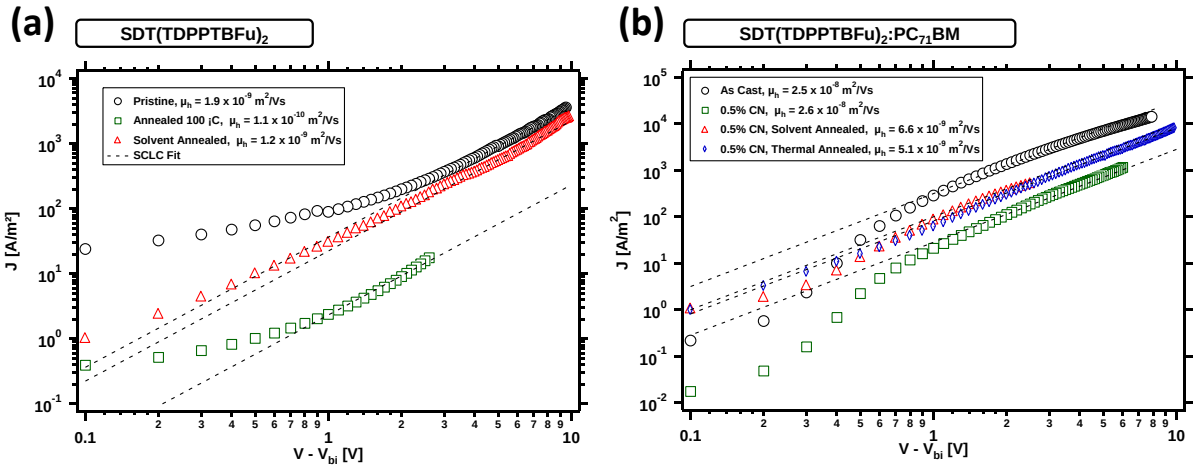

Figure S15. J-V characteristics of hole-only diodes prepared with the architecture of ITO/PEDOT:PSS/$SOHDT_{EH}(TDPP_{EH}TBFu)_2$/Au a) and ITO/PEDOT:PSS/ $SOHDT_{EH}(TDPP_{EH}TBFu)_2$:$PC_{71}BM$/Au b).

5. Thermal annealing of SOHDT(TDPPTBFu)$_2$:$PC_{71}BM$ films

Films of **SOHDT(TDPPTBFu)$_2$**:$PC_{71}BM$ were prepared by spincasting and annealed at temperatures up to 140 ^oC. The results are reported in Figure S16.

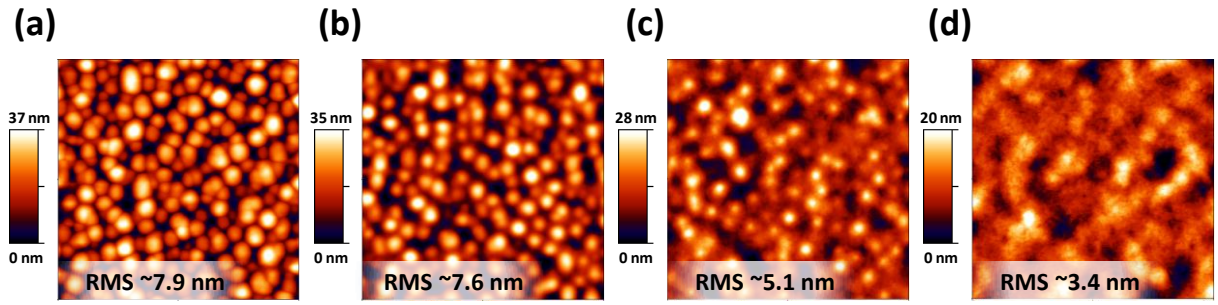

Figure S16. Tapping-mode atomic force microscopy (AFM) height images of SOHDT(TDPPTBFu)$_2$:PC$_{71}$BM films annealed at different temperatures. a) As-cast film, b) annealed at 110 ^{o}C, c) annealed at 120 ^{o}C, d) annealed at 140 ^{o}C. All images are 2μm × 2μm.

6. Solvent additives

6.1. Solvent Additive Properties

A range of solvent additives were explored. Several previously reported solvent additives were chosen (1,8-diodooctane, 1,8-octanedithiol, 1-chloronaphthalene), as well as additives with high dispersive parameters (1,4 diiodobutane, diiodomethane, 1,1,2,2-tetrabromoethane), additives with structural similarities to 1-chloronaphthalene, (1-methylnaphthalene, isoquinoline, decalin) which was observed to provide the larges J_{SC}, the thiophene derivatives 2-bromothiophene and 2-cyanothiophene, the highly polar liquid propylene carbonate and N-methylpyrrolidone, whose structure bears resemblance to diketopyrrolopyrrole. The boiling point, vapor pressure, density and Hansen parameters of each additive are reported in **Table S12**.

Table S12. Solvent additive properties.[a]

Additive	Boiling Point	Vapor Pressure at 25 ^{o}C	Density	δ_D	δ_P	δ_H
	[^{o}C]	[mm Hg]	[g/mL]	[MPa$^{1/2}$]	[MPa$^{1/2}$]	[MPa$^{1/2}$]
1,4-Diiodobutane	195	0.47	2.29	18.9	4.5	5.8
1,8-Diiodooctane	327	-	-	18.1	3.7	4.7

1,8-Octanedithiol	253	0.01	0.96	16.9	6.1	5.8
Diiodomethane	182	1.24	3.25	22	3.9	5.5
1,1,2,2-Tetrabromoethane	244	0.03	2.97	21	7	8.2
Decalin	196	0.78	0.90	17.8	0	0
1-Methyl naphthalene	245	0.05	1.02	19.7	0.8	4.7
Isoquinoline	237	0.05	1.05	19.6	6.2	5.8
2-Bromothionphene	149	4.42	1.68	20.1	5.2	4.6
2-Cyanothiophene	192	-	1.17	19.1	13.1	6.6
Propylene carbonate	242	-	1.19	20	18	4.1
N-Methyl pyrrolidone	204	0.09	1.03	18	12.3	7.2
1-Chloronaphthalene	259	0.02	1.19	20.5	4.9	2.5

[a] All solvent additive properties were taken from S. Abbott , C.M. Hansen Hansen Solubility Parameters in Practice ,(software) Version 3.0.12, **2008–2010** www.hansen-solubility.com (accessed Feb. 2011).

6.2. Morphology of SOHDT(TDPPTBFu)$_2$:PC$_{71}$BM films prepared with solvent additives

AFM images were collected from films prepared with a range of solvent additives, height and phase images are reported in **Figure S17**. Highly dispersive additives with aromatic rings (Naphthalene derivatives and thiophene derivatives) were found to produce relatively smooth films compared to the film with no additive (**Figure S17**a, f). The smoothest films (0.3 nm RMS roughness) were obtained with 1-chloronaphthalene, using 0.5% additive concentration (**Figure S17**b, c), and became only slightly more rough (0.5 nm RMS roughness) upon increasing the additive content to 4% (**Figure S16**g, h). 1-methyl naphthalene (**Figure S17**d, i), isoquinoline (**Figure S17**e, j), 2-bromothiophene (**Figure S17**l, q), and 2-cyanothiophene (**Figure S17**m, r) led to roughness' of 0.5, 0.5, 1.0 and 0.8 nm, respectively. Films prepared from the hydrocarbon decalin (**Figure S17**k, p), or the polar liquids propylene carbonate (**Figure S17**n, s) and N-methylpyrrolidone (**Figure S17** o, t) led to very rough films, with RMS roughnesses of 18, 33 and 21 nm, respectively.

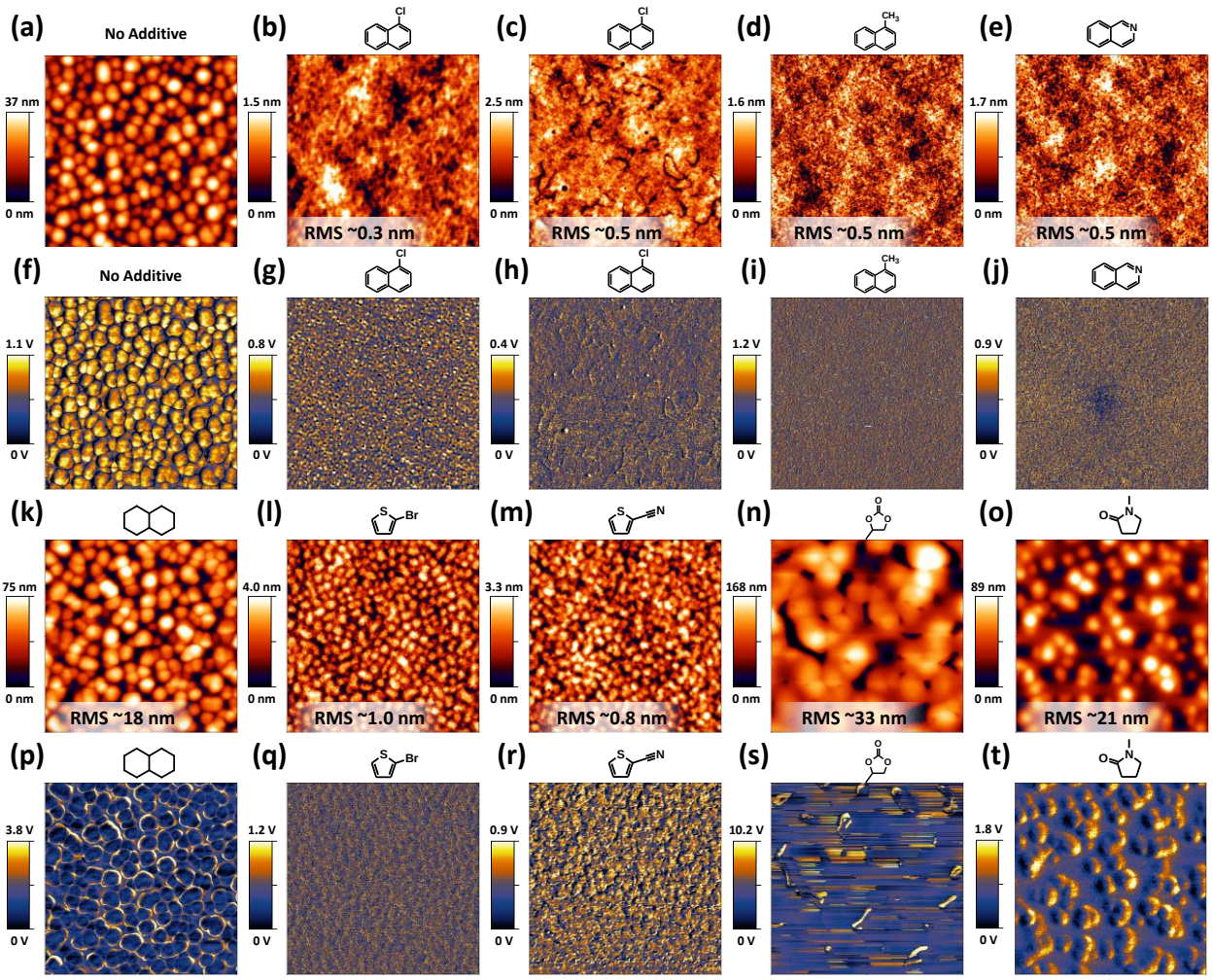

Figure S17. Tapping-mode AFM images of *SOHDT(TDPPTBFu)$_2$:PC$_{71}$BM* films prepared with different solvent additives. Height images are displayed in a)-e) and k)-o) while phase images are shown in f)-j) and p)-t). Additives are displayed in the following order: a), f) no additive; b), c), g), h) chloronapthalene; d), i) 1-methylnaphthalene; e), j) isoquinoline; k), p) decalin; l), q) 2-bromothiophene; m), r) 2-cyanothiophene; n), s) propylene carbonate; o), t) N-methylpyrrolidone. All films were prepared with 0.5% additive in chloroform with the exception of a) and c), in which 0% and 4% additive were used, respectively. All images are 2μm × 2μm.

6.3. J-V characteristics of films prepared with different solvent additives

Solar cells were fabricated using the same films used to collect AFM images in **Figure S17**. The current voltage characteristics are plotted in **Figure S18** and the results are summarized in **Table S13**. A discussion of the devices can be found in the main text.

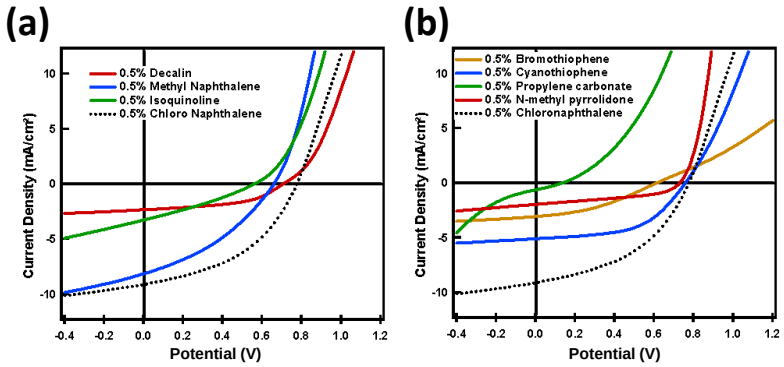

Figure S18. Comparison of J-V characteristics of *SOHDT$_{EH}$(TDPP$_{EH}$TBFu)$_2$:PC$_{71}$BM* devices prepared with decalin, methyl naphthalene, isoquinoline, chloronaphthalene a) as well as bromothiophene, cyanothiophene, propylene carbonate, N-methyl pyrrolidone and chloronaphthalene b).

Table S13. Photovoltaic properties of **SOHDT(TDPPTBFu)$_2$**:PC$_{71}$BM devices prepared with different additives.

Additive	Additive Conc. [%]	Rough-ness [nm]	R_{series} [Ωcm^2]	R_{shunt} [kΩcm^2]	J_{SC} [mV]	V_{OC} [mV]	FF [%]	PCE [%]
No additive	-	8.0	10.3	5.8	2.3	805	47	0.89
1,8-Diiodooctane	2	-	12.9	17	5.3	666	36	1.26
1,8-Octanedithiol	2	-	135	52	0.7	700	21	0.10
Diiodomethane	2	-	26	370	2.4	745	40	0.72
1,1,2,2-Tetrabromoethane	2	-	7.2	4.8	8.9	730	47	3.02
Decalin	0.5	18	-	-	2.3	704	49	0.81
1-Methyl naphthalene	0.5	0.5	6.7	7.6	8.1	659	36	1.93
Isoquinoline	0.5	0.5	5.6	590	3.3	559	30	0.54
2-Bromothionphene	0.5	1.0	58.4	270	3.0	611	37	0.69
2-Cyanothiophene	0.5	0.8	15.5	13	5.1	757	53	2.05
Propylene carbonate	0.5	33	4.5	0.31	0.6	131	28	0.02
N-Methyl pyrrolidone	0.5	21	4.7	46	1.9	728	44	0.62
1-Chloronaphthalene	0.25	-	-	-	8.5	842	40	2.86
1-Chloronaphthalene	0.5	0.3	10.5	13	9.5	834	46	3.61
1-Chloronaphthalene[a]	0.5	-	9.1	110	9.4	854	47	3.80

1-Chloronaphthalene	1	-	-	-	9.0	803	40	2.85
1-Chloronaphthalene	2	-	-	-	9.1	821	38	2.85
1-Chloronaphthalene	4	0.4	-	-	9.0	829	40	2.99

[a] Annealed at 80 ^{o}C.

7. Repeatability

Devices were prepared using identical conditions (0.5% CN, 1750 rpm, annealed at 80 ^{o}C) on 5 different occasions between Feb and May 2011. The current voltage characteristics are plotted in **Figure S19**. The current-voltage characteristics show good repeatability, with a J_{SC} of 9.4 ± 0.25 mA/cm^2, a V_{OC} of 847 ± 5 mV, a FF of 47.9 ± 1.1% and a PCE of 3.79 ± 0.045%.

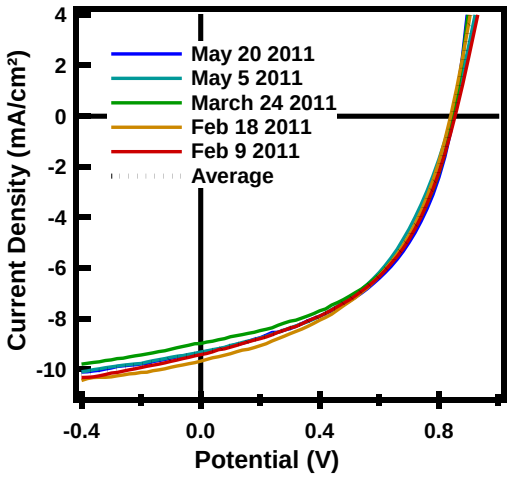

Figure S19. Comparison of J-V characteristics of *SOHDT$_{EH}$(TDPP$_{EH}$TBFu)$_2$:PC$_{71}$BM* devices prepared with 0.5% chloronaphthalene and annealed at 80 ^{o}C on different dates.

8. Alternative solvents and solvent vapor annealed (SVA) films

In an attempt to control the morphology of SOHDT$_{EH}$(TDPP$_{EH}$TBFu)$_2$:PC$_{71}$BM films, many techniques were explored including the use of solvents other than chloroform. It was observed that using 1,2-dichlorobenzene as a solvent or solvent vapor annealing with 1,2-dichlorobenzene yielded a morphology with crystal-like features apparent in AFM images (**Figure S20)**. The crystallinity of the films was confirmed by XRD, an X-ray diffractogram taken from a film spincast from 1,2-dichlorobenzene is shown in **Figure S21**. The presence of a diffraction peak indicates that a crystal phase is present with a well-defined d-spacing value. No diffraction peak was observed for SOHDT$_{EH}$(TDPP$_{EH}$TBFu)$_2$:PC$_{71}$BM films prepared with any

solvent additive or after thermal annealing at moderate temperatures. Although the presence of a crystalline phase bodes well for hole transport and the morphology bears some resemblance to the optimized morphology of the DPP(TBFu)$_2$:PC$_{71}$BM system, 1,2-dichlorobenzene could not be used as a solvent for BHJ devices due to inconsistent films and dewetting issues. However, we discovered that a similar morphology and diffraction pattern could be obtained by exposing a SOHDT$_{EH}$(TDPP$_{EH}$TBFu)$_2$:PC$_{71}$BM film prepared with 0.5% CN to 1,2-dichlorobenzene solvent vapors. A diffractogram of such a film after 20 min. exposure to 1,2-dichlorobenzene solvent vapor is included in **Figure S21**.

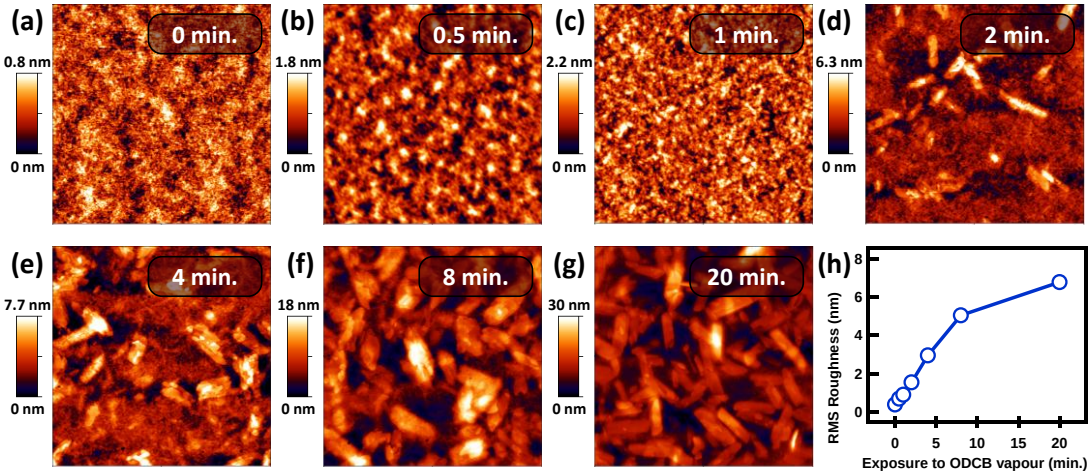

Figure S20. AFM images of films after exposure to ODCB vapor. a) Before exposure. b) After 0.5 minutes. c) After 1 minutes. d) After 2 minutes. e) After 4 minutes. f) After 8 minutes. g) After 20 minutes. h) Plot of roughness vs. exposure to solvent vapor. All images are 5 μm × 5 μm.

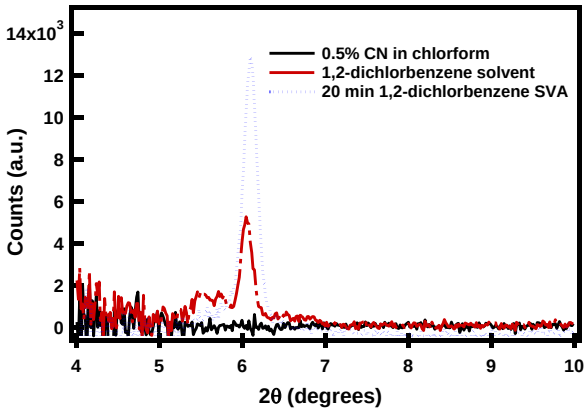

Figure S21. X-ray diffractograms of *SOHDT$_{EH}$(TDPP$_{EH}$TBFu)$_2$:PC$_{71}$BM* films.

Photovoltaic devices were prepared from SOHDT$_{EH}$(TDPP$_{EH}$TBFu)$_2$:PC$_{71}$BM films prepared with 0.5% CN additive and exposed to 1,2-dichlorobenzene solvent vapor for varying lengths of time. The J-V curves are plotted in **Figure S22**. It is interesting to note that despite significant changes in morphology, the J-V characteristics show relatively little variation.

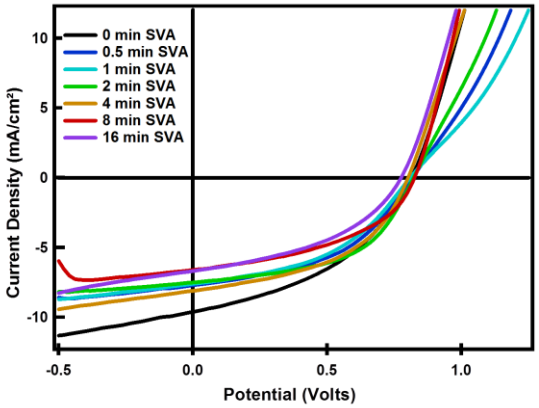

Figure S22. Comparison of J-V characteristics of *SOHDT$_{EH}$(TDPP$_{EH}$TBFu)$_2$:PC$_{71}$BM* devices prepared with 0.5% chloronaphthalene and exposed to 1,2-dicholorobenzene solvent vapor for different lengths of time.

[1] Fargeas, V.; Favresse, F.; Mathieu, D.; Beaudet, I.; Charrue, P.; Lebret, B.; Piteau, M.; Quintard, J. *Eur. J. Org. Chem.* **2003**, *2003*, 1711.

[2] Carey, F. A.; Sundberg, R. J. *Advanced Organic Chemistry Part A: Structure and Mechanisms,* 5th ed.; Springer: New York, 2007; pp 815-816.

[3] J. Zhou, X. Wan, Y. Liu, F. Wang, G. Long, C. Li, Y. Chen *Macromol. Chem. Phys.* **2011**, *212*, 1109.

[4] Tamayo, A. B.; Walker, B.; Nguyen, T.-Q. *J. Phys. Chem. C* **2008**, *112*, 11545.